Elsevier Editorial System(tm) for Colloids and Surfaces B: Biointerfaces
Manuscript Draft

Manuscript Number: COLSUB-D-17-00883R1

Title: A comparison study between electrospun polycaprolactone and piezoelectric poly(3-hydroxybutyrate-co-3-hydroxyvalerate) scaffolds for bone tissue engineering

Article Type: Full Length Article

Keywords: Polymer scaffolds, nanoparticles, cell adhesion, mineralization, electrospinning

Corresponding Author: Mr. Roman Anatolievich Surmenev, Ph.D.

Corresponding Author's Institution: National Research Tomsk Polytechnic University

First Author: Svetlana Gorodzha

Order of Authors: Svetlana Gorodzha; Albert Muslimov; Dina Syromotina; Alexander Timin, Dr; Nikolai Tcvetkov; Kirill Lepik; Aleksandra Petrova; Maria Surmeneva, Dr; Dmitry Gorin, Dr; Gleb Sukhorukov, Dr; Roman Anatolievich Surmenev, Ph.D.

Manuscript Region of Origin: RUSSIAN FEDERATION

Abstract: In this study, bone scaffolds composed of polycaprolactone (PCL), piezoelectric poly(3-hydroxybutyrate-co-3-hydroxyvalerate) (PHBV) and a combination of poly(3-hydroxybutyrate-co-3-hydroxyvalerate) and silicate containing hydroxyapatite (PHBV-SiHA) were successfully fabricated by a conventional electrospinning process. The morphological, chemical, wetting and biological properties of the scaffolds were examined. All fabricated scaffolds are composed of randomly oriented fibres with diameters from 800 nm to 12 μm. Fibre size increased with the addition of SiHA to PHBV scaffolds. Moreover, fibre surface roughness in the case of hybrid scaffolds was also increased. XRD, FTIR and Raman spectroscopy were used to analyse the chemical composition of the scaffolds, and contact angle measurements were performed to reveal the wetting behaviour of the synthesized materials. To determine the influence of the piezoelectric nature of PHBV in combination with SiHA nanoparticles on cell attachment and proliferation, PCL (non-piezoelectric), pure PHBV, and PHBV-SiHA scaffolds were seeded with human mesenchymal stem cells (hMSCs). In vitro study on hMSC adhesion, viability, spreading and osteogenic differentiation showed that the PHBV-SiHA scaffolds had the largest adhesion and differentiation abilities compared with other scaffolds. Moreover, the piezoelectric PHBV scaffolds have demonstrated better calcium deposition potential compared with non-piezoelectric PCL. The results of the study revealed pronounced advantages of hybrid PHBV-SiHA scaffolds to be used in bone tissue engineering.

Response to Reviewers: Dear Editor,
We thank the Editor and Referees for valuable comments what we found very useful to improve the manuscript. The Referees have brought up important

points which have been carefully considered by us while making a revision. We revised the text, modified figures, added the experimental data and extended discussion as well. Herein, we explain how we revised the paper based on those comments and recommendations. All changes are marked in yellow in the revised version of manuscript. Please, find below our point-to-point answers to these comments with addressing to correspondent changes made in the manuscript.
Yours sincerely,
Corresponding author on behalf of all authors
Associate Professor Dr. Roman Surmenev

1. REVIEWER'S COMMENT: For the scaffold fabrication section (page 5, 2.2), composite PHBV-SiHA scaffolds were fabricated. The bottom picture of Figure 1 showed the morphology of PCL-SiHA. Was there any PCL mixed in the composite scaffolds, and how much of PCL was added?
REPLY: We corrected the mistake which occurred in Fig. 1. No hybrid PCL-SiHA scaffolds were fabricated. We prepared and investigated only the scaffolds of PHBV-SiHA. The details on scaffolds fabrication are available in the manuscript.

2. REVIEWER'S COMMENT: As for the morphology evaluation (page 8, line 11), "Cell morphology was quantified by manually outlining 10 cells per image per group in ImageJ". a sample size of 10 was too small. A larger sample size would be more persuasive to draw a conclusion.
REPLY: In our work, using ImageJ software we analyzed 10 cells per image. The overlay number of evaluated images was 10 which were taken in different places of scaffolds. With respect to reviewer's comments, we have changed the manuscript, describing the process for analyzing cell morphology more clearly. Please, find this modification on page 8 marked in yellow.
3. REVIEWER'S COMMENT: For cell proliferation test (page 9, line 4), the scaffolds were cut into size of 1*1 cm2, while the bottom size of 24 well-plate was about 15 mm in diameter. So the bottoms were not entirely covered by scaffolds. How to make sure the same number of cells were seeded on the scaffolds?
REPLY: For cell proliferation test, the initial number of hMSCs was the same for all wells, where 1*1 cm2 scaffold were located. During the cell adhesion analysis, different number of cells were adherent on scaffolds (PCL, PHBV and PHBV-SiHA), as shown in Fig 3A. Therefore, the different number of cells were adherent on scaffold surface after 24 h incubation. The aim of this research was to confirm whether all types of scaffolds provide cell growth during a long-term cultivation. We evaluated them qualitatively using confocal microscopy analysis without quantitative comparison of cell proliferative potential between the tested scaffolds.
4. REVIEWER'S COMMENT: In page 12, line 25, it was noticed that "the incorporation of SiHA nanoparticles into the polymer structure resulted in the increase of the surface roughness". please describe how surface roughness was evaluated and explain why increased roughness resulted in no change of scaffold wettability.
REPLY: The water contact angle measurements were performed to provide understanding on the influence of SiHA nanoparticles on the polymer scaffolds' chemistry and wettability. The water contact angles are shown in Fig. 2 (bottom right). All fibrous samples demonstrate contact angles of over 100o, which reveals the hydrophobic nature of the scaffolds. The largest contact angle is obtained for PCL scaffold (132.13±1.95o) compared with PHBV scaffold and hybrid scaffold of PHBV with SiHA

nanoparticles. It was concluded that the presence of SiHA nanoparticles in the PHBV fibrous scaffold had no significant effect on the contact angle. The contact angle for PHBV-SiHA slightly increased to 125.36±1.61o compared with PHBV (122.55±2.29o). It was expected that due to hydrophilic nature of SiHA nanoparticles used to prepare hybrid scaffolds, the contact angle will be lower for PHBV-SiHA scaffold compared with PHBV. However, due to wettability results obtained in this study, we assume that one of the crucial parameters such as scaffolds porosity and fibers roughness can cause the most pronounced influence on scaffolds wettability. It is reported that the surface roughness increases with fiber diameter increase and additional content of inorganic inclusions such as HA [Xu, C., F. Yang, S. Wang, S. Ramakrishna, In vitro study of human vascular endothelial cell function on materials with various surface roughness. Journal of Biomedical Materials Research A, 2004. 71(1): p. 154-161.; Xu, C., F. Yang, S. Wang, S. Ramakrishna, In vitro study of human vascular endothelial cell function on materials with various surface roughness. Journal of Biomedical Materials Research A, 2004. 71(1): p. 154-161]. According to Fig. 1 (bottom), it can be clearly seen that the presence of SiHA nanoparticles and their agglomerates in the polymer changes the roughness of the fiber surface and creates nanoscale structures, which distort the form and diameter of the fibers [Hassan, M.I., Sultana N., Hamdan S., Bioactivity assessment of poly (ε-caprolactone)/hydroxyapatite electrospun fibers for bone tissue engineering application. Journal of Nanomaterials, 2014. 2014: p. 8.; Gert, H., N Foley, D Zwaan, BJ Kooi, G Palasantzas Roughness controlled superhydrophobicity on single nanometer length scale with metal nanoparticles. RSC Advances, 2015. 5(36): p. 28696-28702.]. Since SiHA is hydrophilic and its content does not exceed 10 wt. %, there is only a negligible change of the contact angle for the scaffolds compositions investigated in this paper. The required changes are done in the manuscript on pp. 12-13.

5. REVIEWER'S COMMENT: In page 15, line 11, "PHBV-SiHA revealed the largest viability of hMSCs (>95%)". Was there any statistical differences between each group? If yes, please mark an error bar on figure 3B.

REPLY: With respect to reviewer comments, we have added statistical difference in figure 5 (bottom-right graph).

6. REVIEWER'S COMMENT: In figure 4, hMSCs on PHBV scaffolds showed nearly spherical shape, while PHBV-SiHA group showed more spreading morphology. The authors did not explain the difference when these two kinds of scaffolds were piezoelectric.

REPLY: The surface charge constant (d33) for the used in the study hybrid polymers were measured. They were revealed to be 0.605±0.093 pC/N and 1.558±0.065 pC/N for PHBV c/l and PHBV c/l +SiHA, respectively. It is known that non-stoichiometric HA also reveals piezoelectric properties [Fukada, E., Yasuda, I., On the piezoelectric effect of bone. Journal of the Physical Society of Japan, 1957. 12: p. 1158-1162], thus we expect that SiHA addition to scaffolds could have contributed in such a way that silicates distorted the lattice of HA which can also generate additional piezoelectric potential in hybrid PHBV-Si-HA scaffolds. Thus, hybrid scaffolds of PHBV-SiHA revealed larger values of d33 constants compared with pure PHBV scaffolds. We also measured the piezocharge constants of PCL, which equaled zero.

Cell culture experiments were performed in static conditions, we expect that the effect of piezoelectric nature of the prepared hybrid compounds is difficult to derive and the most pronounced effect on different cell behavior observed in the paper belongs to SiHA nanoparticles, which addition resulted in both surface chemistry and surface topography changes of the hybrid fiber scaffolds.

7. REVIEWER'S COMMENT: For osteogenic differentiation tests, calcium mineralization was only examined on day 7. To our experience, a longer observation to 14 and 28 days would be more valid to draw a conclusion. And more quantitative evidence would be preferred.
REPLY: There are several variations of protocol for analysis of hMSC osteogenic differentiation. In our research lab, we used the standard protocol for hMSCs osteogenic differentiation, where the evaluation of hMSCs differentiation is performed on day 7. Such a variation of the protocol was also reported in several works [J Microbiol Biotechnol. 2007 Jul;17(7):1113-9. Effects of culture conditions on osteogenic differentiation in human mesenchymal stem cells. Song SJ1, Jeon O, Yang HS, Han DK, Kim BS; Enhanced Osteogenic Differentiation in Zoledronate-Treated Osteoporotic Patients Luca Dalle Carbonare, Monica Mottes, Giovanni Malerba, Antonio Mori, Martina Zaninotto, Mario Plebani, Alessandra Dellantonio and Maria Teresa Valenti Int. J. Mol. Sci. 2017, 18(6), 1261; doi:10.3390/ijms18061261;Regenerative Therapy 2 (2015) 24e31 doi.org/10.1016/j.reth.2015.09.001 Effect of osteogenic differentiation medium on proliferation and differentiation of human mesenchymal stem cells in threedimensional culture with radial flow bioreactor Itsurou Nishimura, Ryuichi Hisanaga, Toru Sato, Taichi Arano, Syuntaro Nomoto, Yoshito Ikada, Masao Yoshinari].
For quantitive evidence of calcium mineralization we used the NIH ImageJ software. In [Gulden Camci-Unal et al. Biomineralization Guided by paper Templates, Scientific Reports, 6, Article number: 27693], it was demonstrated that this software can be used for quantitive analysis of calcium mineralization.
8. REVIEWER'S COMMENT: In page 16, line 23, "stained calcein-calcium complexes were accumulated within the cavity of PHBV-SiHA and PHBV". I have no idea where I can find the cavity, please mark in the figures.
REPLY: With respect to reviewer comments, we marked the cavity for all scaffolds in Figure 5. In this research work, the cavity means the area between fibres of scaffolds. Please, find all changes in the revised manuscript (Figure 5).
9. REVIEWER'S COMMENT: In page 17, line 24, the authors think "increasing the surface area are able to stimulate hMSCs to produce bone mineral". It would be contradictory when hMSCs showed more mineral accumulation on PHBV than PCL with smaller and spherical size.
REPLY: In this sentence, we are describing the surface area of materials, which is correlated with the surface roughness. In many works [Design of biomimetic and bioactive cold plasma-modified nanostructured scaffolds for enhanced osteogenic differentiation of bone marrow-derived mesenchymal stem cells. Wang M, Cheng X, Zhu W, Holmes B, Keidar M, Zhang LG Tissue Eng Part A. 2014 Mar; 20(5-6):1060-71; G. Kumar, et al Freeform Fabricated Scaffolds with Roughened Struts that Enhance both Stem Cell Proliferation and Differentiation by Controlling Cell Shape, Biomaterials, 2012, 33(16): 4022 - 4030], it was shown that high surface roughness of scaffolds and wettability enhance osteogenic differentiation of hMSCs on scaffolds. With respect to reviewer comments, we described this issue more clearly and added more references, confirming that statement.
10. REVIEWER'S COMMENT: Mark the error bars on the bottom-right picture of figure 5, if they were statistically different.
REPLY: With respect to reviewer comments, we have added statistical difference in figure 5 (bottom-right graph).

МИНИСТЕРСТВО ОБРАЗОВАНИЯ И НАУКИ РОССИЙСКОЙ ФЕДЕРАЦИИ

634050, г. Томск,
пр. Ленина, 30, ТПУ
Россия

Tomsk Polytechnic University
30, Lenin Avenue,
Tomsk, 634050, Russia

Федеральное государственное бюджетное образовательное учреждение
высшего профессионального образования

**«НАЦИОНАЛЬНЫЙ ИССЛЕДОВАТЕЛЬСКИЙ
ТОМСКИЙ ПОЛИТЕХНИЧЕСКИЙ УНИВЕРСИТЕТ»**

Тел. (382-2) 70-17-79 Факс: (382-2) 56-38-65. УФК по Томской области
р/с 40501810500002000002 в ГРКЦ ГУ Банка России по Томской области г.Томск БИК 046902001
ИНН 7018007264 ТПУ л/с 20656У20990 ОКПО 02069303; E-mail: tpu@tpu.ru

07/08/2017 № 4.9853

Dear Professor J.L. Brash,

thank you very much for editing Colloids and Surfaces B: Biointerfaces. We would like to submit our revised manuscript titled "**A comparison study between electrospun polycaprolactone and piezoelectric poly(3-hydroxybutyrate-co-3-hydroxyvalerate) scaffolds for bone tissue engineering**", for publication as an original paper.

In this study, bone scaffolds composed of polycaprolactone (PCL), piezoelectric poly(3-hydroxybutyrate-co-3-hydroxyvalerate) (PHBV) and a combination of poly(3-hydroxybutyrate-co-3-hydroxyvalerate) and silicate containing hydroxyapatite (PHBV-SiHA) were successfully fabricated by a conventional electrospinning process. The morphological, chemical, wetting and biological properties of the scaffolds were examined. All fabricated scaffolds are composed of randomly oriented fibres with diameters from 800 nm to 12 μm. Fibre size increased with the addition of SiHA to PHBV scaffolds. Moreover, fibre surface roughness in the case of hybrid scaffolds was also increased. XRD, FTIR and Raman spectroscopy were used to analyse the chemical composition of the scaffolds, and contact angle measurements were performed to reveal the wetting behaviour of the synthesized materials. To determine the influence of the piezoelectric nature of PHBV in combination with SiHA nanoparticles on cell attachment and proliferation, PCL (non-piezoelectric), pure PHBV, and PHBV-SiHA scaffolds were seeded with human mesenchymal stem cells (hMSCs). *In vitro* study on hMSC adhesion, viability, spreading and osteogenic differentiation showed that the PHBV-SiHA scaffolds had the largest adhesion and differentiation abilities compared with other scaffolds. Moreover, the piezoelectric PHBV scaffolds have demonstrated better calcium deposition potential compared with non-piezoelectric PCL. The results of the study revealed pronounced advantages of hybrid PHBV-SiHA scaffolds to be used in bone tissue engineering. I would appreciate your kind consideration and hope to receive your favourable reply soon.

Sincerely,
Roman A. Surmenev, Dr., FRSC
Associate Professor, Head of the Centre of Technology,
National Research Tomsk Polytechnic University,
Tel.: +7 903 953 09 69
E-mail: rsurmenev@gmail.com

Dear Editor,

We thank the Editor and Referees for valuable comments what we found very useful to improve the manuscript. The Referees have brought up important points which have been carefully considered by us while making a revision. We revised the text, modified figures, added the experimental data and extended discussion as well. Herein, we explain how we revised the paper based on those comments and recommendations. All changes are marked in yellow in the revised version of manuscript. Please, find below our point-to-point answers to these comments with addressing to correspondent changes made in the manuscript.

Yours sincerely,

Corresponding author on behalf of all authors

Associate Professor Dr. Roman Surmenev

1. REVIEWER'S COMMENT: For the scaffold fabrication section (page 5, 2.2), composite PHBV-SiHA scaffolds were fabricated. The bottom picture of Figure 1 showed the morphology of PCL-SiHA. Was there any PCL mixed in the composite scaffolds, and how much of PCL was added?

REPLY: We corrected the mistake which occurred in Fig. 1. No hybrid PCL-SiHA scaffolds were fabricated. We prepared and investigated only the scaffolds of PHBV-SiHA. The details on scaffolds fabrication are available in the manuscript.

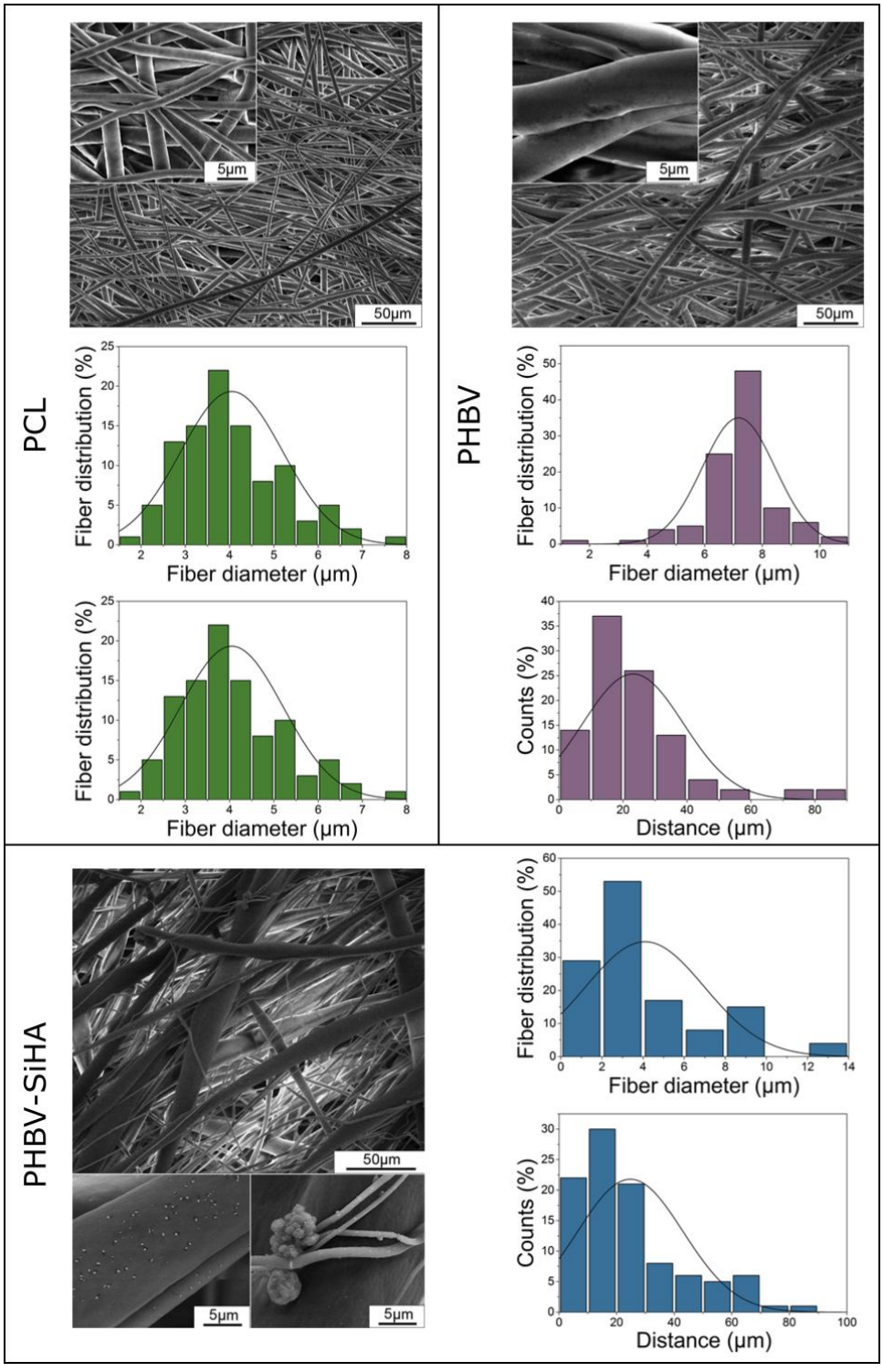
PCL
PHBV
PHBV-SiHA
5μm
50μm
Fiber distribution (%)
Fiber diameter (μm)
Counts (%)
Distance (μm)

2. REVIEWER'S COMMENT: As for the morphology evaluation (page 8, line 11), "Cell morphology was quantified by manually outlining 10 cells per image per group in ImageJ". a sample size of 10 was too small. A larger sample size would be more persuasive to draw a conclusion.

REPLY: In our work, using ImageJ software we analyzed 10 cells per image. The overlay number of evaluated images was 10 which were taken in different places of scaffolds. With respect to reviewer's comments, we have changed the manuscript, describing the process for analyzing cell morphology more clearly. Please, find this modification on page 8 marked in yellow.

3. REVIEWER'S COMMENT: For cell proliferation test (page 9, line 4), the scaffolds were cut into size of 1*1 cm2, while the bottom size of 24 well-plate was about 15 mm in diameter. So the bottoms were not entirely covered by scaffolds. How to make sure the same number of cells were seeded on the scaffolds?

REPLY: For cell proliferation test, the initial number of hMSCs was the same for all wells, where 1*1 cm2 scaffold were located. During the cell adhesion analysis, different number of cells were adherent on scaffolds (PCL, PHBV and PHBV-SiHA), as shown in Fig 3A. Therefore, the different number of cells were adherent on scaffold surface after 24 h incubation. The aim of this research was to confirm whether all types of scaffolds provide cell growth during a long-term cultivation. We evaluated them qualitatively using confocal microscopy analysis without quantitative comparison of cell proliferative potential between the tested scaffolds.

4. REVIEWER'S COMMENT: In page 12, line 25, it was noticed that "the incorporation of SiHA nanoparticles into the polymer structure resulted in the increase of the surface roughness". please describe how surface roughness was evaluated and explain why increased roughness resulted in no change of scaffold wettability.

REPLY: The water contact angle measurements were performed to provide understanding on the influence of SiHA nanoparticles on the polymer scaffolds' chemistry and wettability. The water contact angles are shown in Fig. 2 (bottom right). All fibrous samples demonstrate contact angles of over 100^{o}, which reveals the hydrophobic nature of the scaffolds. The largest contact angle is obtained for PCL scaffold (132.13 ± 1.95^{o}) compared with PHBV scaffold and hybrid scaffold of PHBV with SiHA nanoparticles. It was concluded that the presence of SiHA nanoparticles in the PHBV fibrous scaffold had no significant effect on the contact angle. The

contact angle for PHBV-SiHA slightly increased to 125.36±1.61^{o} compared with PHBV (122.55±2.29^{o}). It was expected that due to hydrophilic nature of SiHA nanoparticles used to prepare hybrid scaffolds, the contact angle will be lower for PHBV-SiHA scaffold compared with PHBV. However, due to wettability results obtained in this study, we assume that one of the crucial parameters such as scaffolds porosity and fibers roughness can cause the most pronounced influence on scaffolds wettability. It is reported that the surface roughness increases with fiber diameter increase and additional content of inorganic inclusions such as HA [Xu, C., F. Yang, S. Wang, S. Ramakrishna, *In vitro study of human vascular endothelial cell function on materials with various surface roughness.* Journal of Biomedical Materials Research A, 2004. **71**(1): p. 154-161.; Xu, C., F. Yang, S. Wang, S. Ramakrishna, *In vitro study of human vascular endothelial cell function on materials with various surface roughness.* Journal of Biomedical Materials Research A, 2004. **71**(1): p. 154-161]. According to Fig. 1 (bottom), it can be clearly seen that the presence of SiHA nanoparticles and their agglomerates in the polymer changes the roughness of the fiber surface and creates nanoscale structures, which distort the form and diameter of the fibers [Hassan, M.I., Sultana N., Hamdan S., *Bioactivity assessment of poly (ε-caprolactone)/hydroxyapatite electrospun fibers for bone tissue engineering application.* Journal of Nanomaterials, 2014. **2014**: p. 8.; Gert, H., N Foley, D Zwaan, BJ Kooi, G Palasantzas *Roughness controlled superhydrophobicity on single nanometer length scale with metal nanoparticles.* RSC Advances, 2015. **5**(36): p. 28696-28702.]. Since SiHA is hydrophilic and its content does not exceed 10 wt. %, there is only a negligible change of the contact angle for the scaffolds compositions investigated in this paper. The required changes are done in the manuscript on pp. 12-13.

5. REVIEWER'S COMMENT: In page 15, line 11, "PHBV-SiHA revealed the largest viability of hMSCs (>95%)". Was there any statistical differences between each group? If yes, please mark an error bar on figure 3B.

REPLY: With respect to reviewer comments, we have added statistical difference in figure 5 (bottom-right graph).

6. REVIEWER'S COMMENT: In figure 4, hMSCs on PHBV scaffolds showed nearly spherical shape, while PHBV-SiHA group showed more spreading morphology. The authors did not explain the difference when these two kinds of scaffolds were piezoelectric.

REPLY: The surface charge constant (d_{33}) for the used in the study hybrid polymers were measured. They were revealed to be 0.605±0.093 pC/N and 1.558±0.065 pC/N for PHBV c/l and PHBV c/l +SiHA, respectively. It is known that non-stoichiometric HA also reveals piezoelectric properties [Fukada, E., Yasuda, I., *On the piezoelectric effect of bone*. Journal of the Physical Society of Japan, 1957. **12**: p. 1158-1162], thus we expect that SiHA addition to scaffolds could have contributed in such a way that silicates distorted the lattice of HA which can also generate additional piezoelectric potential in hybrid PHBV-Si-HA scaffolds. Thus, hybrid scaffolds of PHBV-SiHA revealed larger values of d_{33} constants compared with pure PHBV scaffolds. We also measured the piezocharge constants of PCL, which equaled zero.

Cell culture experiments were performed in static conditions, we expect that the effect of piezoelectric nature of the prepared hybrid compounds is difficult to derive and the most pronounced effect on different cell behavior observed in the paper belongs to SiHA nanoparticles, which addition resulted in both surface chemistry and surface topography changes of the hybrid fiber scaffolds.

7. **REVIEWER'S COMMENT:** For osteogenic differentiation tests, calcium mineralization was only examined on day 7. To our experience, a longer observation to 14 and 28 days would be more valid to draw a conclusion. And more quantitative evidence would be preferred.

REPLY: There are several variations of protocol for analysis of hMSC osteogenic differentiation. In our research lab, we used the standard protocol for hMSCs osteogenic differentiation, where the evaluation of hMSCs differentiation is performed on day 7. Such a variation of the protocol was also reported in several works [*J Microbiol Biotechnol. 2007 Jul;17(7):1113-9. Effects of culture conditions on osteogenic differentiation in human mesenchymal stem cells. Song SJ1, Jeon O, Yang HS, Han DK, Kim BS; Enhanced Osteogenic Differentiation in Zoledronate-Treated Osteoporotic Patients Luca Dalle Carbonare, Monica Mottes, Giovanni Malerba, Antonio Mori, Martina Zaninotto, Mario Plebani, Alessandra Dellantonio and Maria Teresa Valenti Int. J. Mol. Sci. 2017, 18(6), 1261; doi:10.3390/ijms18061261;Regenerative Therapy 2 (2015) 24e31 doi.org/10.1016/j.reth.2015.09.001 Effect of osteogenic differentiation medium on proliferation and differentiation of human mesenchymal stem cells in threedimensional culture with radial*

flow bioreactor Itsurou Nishimura, Ryuichi Hisanaga, Toru Sato, Taichi Arano, Syuntaro Nomoto, Yoshito Ikada, Masao Yoshinari].

For quantitive evidence of calcium mineralization we used the NIH ImageJ software. In [*Gulden Camci-Unal et al. Biomineralization Guided by paper Templates, Scientific Reports, 6, Article number: 27693*], it was demonstrated that this software can be used for quantitive analysis of calcium mineralization.

8. REVIEWER'S COMMENT: In page 16, line 23, "stained calcein-calcium complexes were accumulated within the cavity of PHBV-SiHA and PHBV". I have no idea where I can find the cavity, please mark in the figures.

REPLY: With respect to reviewer comments, we marked the cavity for all scaffolds in Figure 5. In this research work, the cavity means the area between fibres of scaffolds. Please, find all changes in the revised manuscript (Figure 5).

9. REVIEWER'S COMMENT: In page 17, line 24, the authors think "increasing the surface area are able to stimulate hMSCs to produce bone mineral". It would be contradictory when hMSCs showed more mineral accumulation on PHBV than PCL with smaller and spherical size.

REPLY: In this sentence, we are describing the surface area of materials, which is correlated with the surface roughness. In many works [Design of biomimetic and bioactive cold plasma-modified nanostructured scaffolds for enhanced osteogenic differentiation of bone marrow-derived mesenchymal stem cells. Wang M, Cheng X, Zhu W, Holmes B, Keidar M, Zhang LG Tissue Eng Part A. 2014 Mar; 20(5-6):1060-71; G. Kumar, et al Freeform Fabricated Scaffolds with Roughened Struts that Enhance both Stem Cell Proliferation and Differentiation by Controlling Cell Shape, Biomaterials, 2012, 33(16): 4022 - 4030], it was shown that high surface roughness of scaffolds and wettability enhance osteogenic differentiation of hMSCs on scaffolds. With respect to reviewer comments, we described this issue more clearly and added more references, confirming that statement.

10. REVIEWER'S COMMENT: Mark the error bars on the bottom-right picture of figure 5, if they were statistically different.

REPLY: With respect to reviewer comments, we have added statistical difference in figure 5 (bottom-right graph).

***Highlights (for review)**

- Poly(3-hydroxybutyrate-co-3-hydroxyvalerate) scaffolds with SiHA were investigated
- Piezoelectric scaffolds with SiHA stimulated adhesion and differentiation of hMSCs
- Piezoelectric scaffolds revealed superior osteoinductive properties
- Piezoelectric scaffolds demonstrated significantly better calcium deposition potential

Graphical Abstract

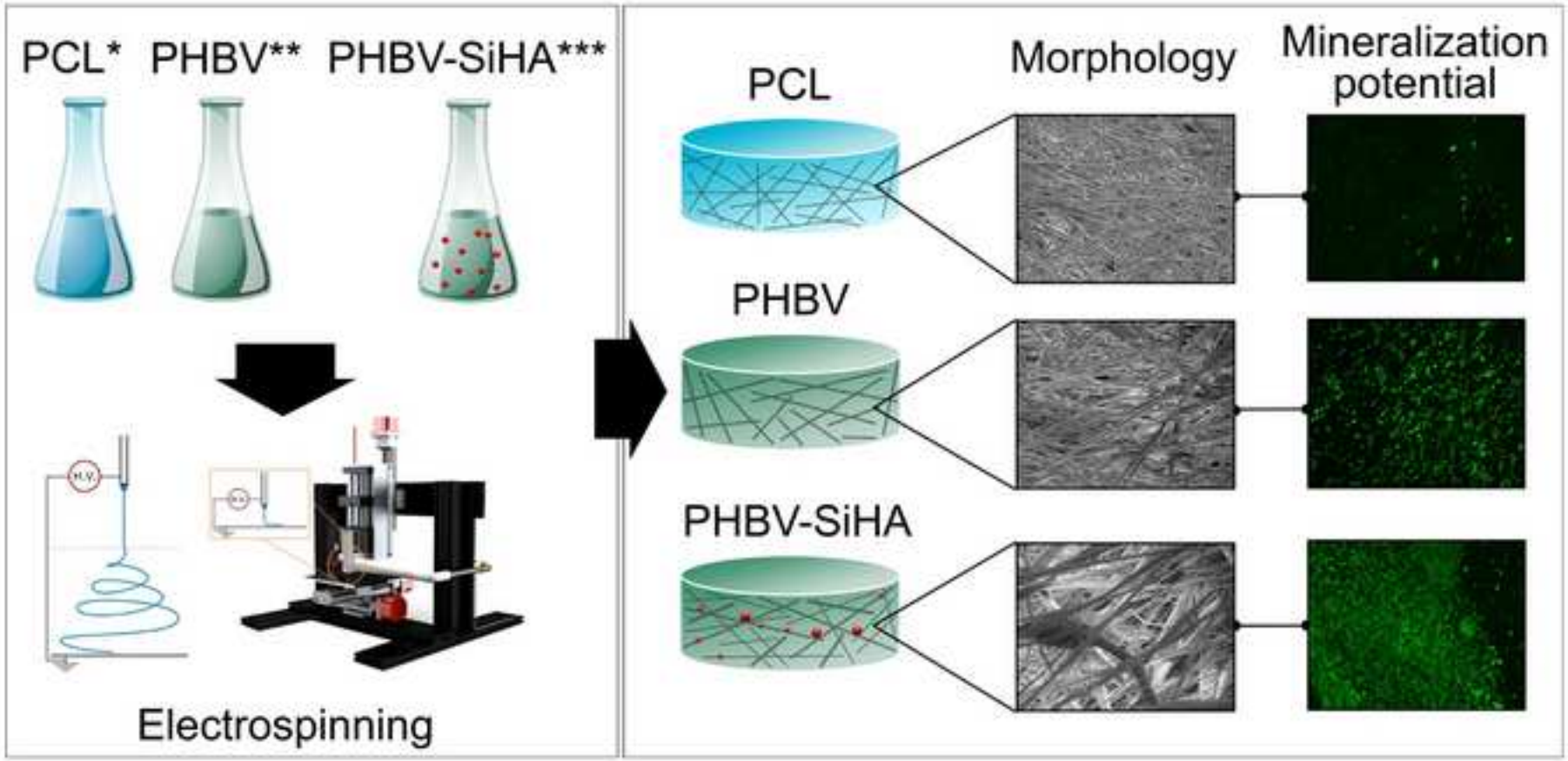

PCL* - Polycaprolactone
PHBV** - Poly(3-Hydroxybutyrate-co-3-Hydroxyvalerate)
SiHA*** - Silicate-containing Hydroxyapatite

A short statistical summary of the article:

- total number of words – 7644

- total number tables/figures – 0/5

A comparison study between electrospun polycaprolactone and piezoelectric poly(3-hydroxybutyrate-co-3-hydroxyvalerate) scaffolds for bone tissue engineering

Svetlana N. Gorodzha[1], Albert R. Muslimov[2], Dina S. Syromotina[1,3], Alexander S. Timin[3], Nikolai Y. Tcvetkov[4], Kirill V. Lepik[4], Aleksandra V. Petrova[4], Maria A. Surmeneva[1], Dmitry A. Gorin[3,5], Gleb B. Sukhorukov[3,6], Roman A. Surmenev[1*]

[1]Experimental Physics Department, National Research Tomsk Polytechnic University, Lenin Avenue, 30, 634050, Tomsk, Russian Federation

[2]First I. P. Pavlov State Medical University of St. Petersburg, Lev Tolstoy str., 6/8, 197022, Saint-Petersburg, Russian Federation

[3]RASA Center in Tomsk, National Research Tomsk Polytechnic University, Lenin Avenue, 30, 634050, Tomsk, Russian Federation

[4]Research Institute of Influenza, Popova str., 15/17, 197376, Saint-Petersburg, Russian Federation

[5]Saratov State University, Saratov, Russian Federation

[6]School of Engineering and Materials Science, Queen Mary University of London, Mile End Road, London E1 4NS, United Kingdom.

Correspondence to Associate Prof. Dr Roman Surmenev at rsurmenev@mail.ru

Abstract

In this study, bone scaffolds composed of polycaprolactone (PCL), piezoelectric poly(3-hydroxybutyrate-co-3-hydroxyvalerate) (PHBV) and a combination of poly(3-hydroxybutyrate-co-3-hydroxyvalerate) and silicate containing hydroxyapatite (PHBV-SiHA) were successfully fabricated by a conventional electrospinning process. The morphological, chemical, wetting and biological properties of the scaffolds were examined. All fabricated scaffolds are composed of randomly oriented fibres with diameters from 800 nm to 12 μm. Fibre size increased with the addition of SiHA to PHBV scaffolds. Moreover, fibre surface roughness in the case of hybrid scaffolds was also increased. XRD, FTIR and Raman spectroscopy were used to analyse the chemical composition of the scaffolds, and contact angle measurements were performed to reveal the wetting behaviour of the synthesized materials. To determine the influence of the piezoelectric nature of PHBV in combination with SiHA nanoparticles on cell attachment and proliferation, PCL (non-piezoelectric), pure PHBV, and PHBV-SiHA scaffolds were seeded with human mesenchymal stem cells (hMSCs). *In vitro* study on hMSC adhesion, viability, spreading and osteogenic differentiation showed that the PHBV-SiHA scaffolds had the largest adhesion and differentiation abilities compared with other scaffolds. Moreover, the piezoelectric PHBV scaffolds have demonstrated better calcium deposition potential compared with non-piezoelectric PCL. The results of the study revealed pronounced advantages of hybrid PHBV-SiHA scaffolds to be used in bone tissue engineering.

Keywords: Polymer scaffolds, nanoparticles, cell adhesion, mineralization, electrospinning

1. Introduction

The concept of bone defect repair using three dimensional (3D) tissue scaffolds is becoming increasingly promising in regenerative medicine [1]. The ability of bone to remodel, coupled

with the capacity of some polymers to biodegrade, allows bone tissue to regenerate completely in place of the implanted material, which is the evidence of successful bone treatment [2]. It is known that bone is a complex tissue with various functions and properties in the body to reproduce it in the laboratory approach. Therefore, the main aim of biomaterials was, and still is, to create a three-dimensional (3D) scaffold to stimulate the remarkable regenerative capacity of bone.

Electrospinning is an appropriate method for 3D scaffold fabrication due to its capability to create nano- and micro-scale structured materials with variable fibre diameters and porosity that imitate the porous structure of the bone [3]. It is important to note that scaffolds should have a desirable pore size to achieve sufficient vascularization and deliver nutrients, which, in its turn, facilitates improved proliferation and osteoblastic differentiation of human bone cells [4]. At the same time, the morphology of electrospun scaffolds should establish high cell adhesion and proliferation that can be controlled by the fibre diameter and topography of the fibres. Therefore, for cell adhesion, an optimal range of fibre diameter of the scaffolds exists, which may vary in the range from several tens of nanometres to a few microns [5] depending on the cell type and tissue.

Electrospun scaffolds can be prepared based on a wide range of polymers. There are a variety of natural and synthetic materials with various structure and properties that are potential biomaterials for biomedical and tissue engineering. Synthetic polymers are more preferable materials for regenerative medicine than natural because they are easier to process and can be tailored to give a wider range of mechanical properties. One of the most frequently used synthetic polymers is polycaprolactone (PCL), which has suitable mechanical and biodegradable properties for the development of functional hybrid scaffolds [6]. Some polymers such as poly(lactic acid) (PLA), polyhydroxyalkanoate (PHA), polyvinylidene fluoride (PVDF) have a specific piezoelectric property. These materials especially attract attention due to their

piezoelectricity, which is inherent in different living tissues of the human body, including bone [7].

The first reference to the piezoelectric properties of the bone was reported in 1954 [8]. Later, the piezoelectric properties of bone had attracted interest due to the bone regeneration process [9]. It was discovered that the mechanical stress in bone produces electrical signals, and these signals represent the stimulus that promotes bone growth and remodelling according to Wolff's law [10].

After the discovery of piezoelectricity in poly(3-hydroxybutyrate-co-3-hydroxyvalerate) (PHBV) in 1986, this polymer was highlighted among all piezoelectric polymers, because it had the most similar piezoelectric coefficient to those of the natural bone [11]. These properties, combined with its biocompatibility and biodegradation, inspired scientists to attempt to use this polymer as a bone substitute with the capability to mimic the piezoelectricity of natural bone.

The applications of PHBV scaffolds could be extended considerably if bone growth and healing are stimulated. It is well known that synthetic hydroxyapatite (HA) is similar to the mineral component of natural bone and possesses osteoconductivity to promote osteogenesis (bone growth). Recently, the HA nanoparticles were widely used to impart useful properties to polymer scaffolds. It was reported that biodegradable hybrid scaffolds containing HA particles possessed osteoconductive properties [12]. Furthermore, silicon-containing hydroxyapatite (SiHA) especially, is known to markedly enhance *in vitro* cell proliferation, adhesion [13] and bone tissue growth *in vivo* [14]. However, to the best of our knowledge, there are no papers devoted to studying piezoelectric scaffolds with SiHA additives and revealing the effect of SiHA nanoparticles on cell adhesion and differentiation. Based on piezoelectric polymers and the bioactive characteristics of synthetic SiHA nanoparticles, we decided to combine the advantages of these materials in a single hybrid scaffold.

Thus, this study aimed to develop 3D hybrid scaffolds based on piezoelectric PHBV with the addition of SiHA nanoparticles using an electrospinning technique. A comparison of the morphology, chemical structure, wettability and cell response was performed for different types of 3D scaffolds: non-piezoelectric PCL (control), piezoelectric PHBV and a combination of PHBV-SiHA. Human mesenchymal stem cells (hMSCs) were chosen to study cell adhesion and subsequent differentiation *in vitro*. Due to their unique capability to differentiate into osteoblasts, MSCs allow us to mimic the process of bone grow *in vitro*.

2. Materials and Methods

2.1. Materials

Polymers of polycaprolactone (PCL, M_n = 80,000 g·mol^{-1}) and poly(3-hydroxybutyrate-co-3-hydroxyvalerate) with 12 % valerate fraction (PHBV, M_n = 530,000 g·mol^{-1}) as well as chloroform as a solvent were purchased from Sigma-Aldrich (USA). SiHA, ($Ca_{10}(PO_4)_{5.2}(SiO_4)_{0.8}(OH)_{1.2}$) nanoparticles were obtained as a precursor powder from the Institute of Solid State Chemistry and Mechanochemistry SB RAS (Russia). The SiHA nanoparticles size was in the range 50-100 nm [15].

2.2. Scaffold fabrication

In this study, micro-fibres were prepared via a conventional electrospinning setup developed at National Research Tomsk Polytechnic University, Russia. The objective of the study was to prepare and investigate pure PCL, PHBV polymer scaffolds, and composite scaffolds of PHBV and SiHA nanoparticles. For this, PCL and PHBV polymers were dissolved at a concentration of 9 % and 23 % (w/v), respectively. For the fabrication of composite PHBV-SiHA scaffolds, PHBV solution was mixed with 10 wt. % of SiHA nanoparticles. All the samples were continuously stirred at room temperature for 180 min followed by magnetic stirring for 30 min to

avoid the formation of agglomerates. Polymer solution was loaded into a 10 mL plastic syringe connected with a blunt stainless steel needle (inner diameter 0.58 mm) with a tip connected to the anode. The needle was kept at a voltage of 7 kV. The polymer solution was extruded at a rate of 2 $ml \cdot h^{-1}$ for one hour with the help of a syringe pump (AJ-5803, Angel Electronic Equipment Co., China). The drum collector was mounted at a distance of 5 cm, and the fibres were deposited at a rotation speed of 600 rpm. Once optimal parameters for the preparation of PCL polymer solution were determined, PHBV and PHBV-SiHA fibrous scaffolds were prepared.

Viscosity (μ) measurements used to characterize polymer solutions were performed using a rheometer (MCR301, Anton Paar, Austria) equipped with a concentric cylinder geometry with a diameter of 30 mm, horizontal gap of 1 mm, run with a vertical gap of 1 mm. The shear rate was recorded point by point 20 times.

2.3. Scaffold characterization

Scanning electron microscopy (SEM) (Quanta 200, FEI, Netherlands) was used to characterize the scaffolds' morphology. The samples were coated with gold and examined at an accelerating voltage of 10 kV and magnification of 1,000x and 15,000x. SEM images were analysed by image analysis software (ImageJ, National Institutes of Health, USA). The average fibre diameter and the distance between nearby fibres was determined from approximately 100 random measurements using three images.

Attenuated total reflectance Fourier transform infrared (FTIR) spectroscopy (Tensor-27, Bruker, USA) and Raman spectroscopy (Renishaw Invia Basis, Renishaw, United Kingdom) were used to characterize the chemical bonding structures. For FTIR spectroscopy, 64 scans were collected in the wavelength range from 525 to 4000 cm^{-1} with a resolution of 4 cm^{-1}. A Raman microscope system with two lasers emitting at 532 nm and 785 nm was employed to collect the spectra. For this study, the 532 nm laser was used, and the spectra were collected in extensive mode ranging

from 500 to 3000 cm^{-1}. In this paper, only the most informative peaks from 525 to 2000 cm^{-1} are shown.

X-ray diffraction (XRD) with CuK_{α} radiation (λ=0.154 nm) (XRD-7000, Shimadzu, Japan) was used to investigate the crystallographic structure of the scaffolds. XRD patterns were recorded in the 2θ range from 10° to 60° with a scan speed of 2.0°/min, sampling pitch of 0.03°, preset time of 5.0 sec at 30 kV and 30 mA.

The water contact angle was measured to investigate the wetting behaviour of the scaffolds. The analysis was assessed using static contact angle measurements and performed using drop shape analysis (OCA 15 Plus, Data Physics Instruments GmbH, Germany). Ten droplets (2 $\mu L \cdot s^{-1}$) were seeded on the surfaces of three samples of each studied materials with the size of 2 × 5 cm^2, and the resulting average contact angle was calculated.

2.4. Statistical analysis

All results are expressed as a mean ± standard deviation and have been determined using Student's test for the calculations of the statistical significance.

2.5. Biological evaluation of the obtained scaffolds

2.5.1. Preparation of hMSC culture

Human mesenchymal stem cells (hMSCs) were derived from the bone marrow of healthy donors who gave their informed consent. Cells were isolated using a direct plating procedure. Briefly, 1 mL of whole bone marrow, heparinized, was re-suspended in alpha-MEM (Lonza, Switzerland); supplemented with 100 IU/ml penicillin, 0.1 mg/ml streptomycin (Biolot, Russia), and 10 % FBS (HyClone, USA) and 2 mM Ultraglutamin I (Lonza, Switzerland). The hMSCs were cultured in DMEM under standard cell culture conditions (i.e., 37° C, 5 %/95 % CO_2/air, humidified sterile environment) to > 85 % confluency. Subsequently, hMSCs were detached using trypsin (Sigma-

Aldrich, UK) and passaged up to the second passage (P2) for culture with scaffolds (PCL, PHBV and PHBV-SiHA).

2.5.2. Evaluation of hMSC morphology and adhesion

hMSC morphology and adhesion on the surface of the samples was evaluated at 24 h of incubation. To evaluate cell morphology, hMSCs were seeded at 1.5×10^5 cell per well onto PCL, PHBV and PHBV-SiHA with their size (1×1 cm^2) in a 24-well plate (n = 3). After 24 h incubation at standard culture conditions, hMSCs were washed twice in 1 mL of Dulbecco's phosphate buffered saline (PBS) and incubated with anti-CD90-phycoerythrin (anti-CD90-PE) for 20 min in the dark. Then, the scaffolds with cells were viewed under Confocal Laser Scanning Microscope (CLSM, Carl Zeiss, Germany) with a 40x/1.30 objective. A 488 nm laser was used to excite the anti-CD90-PE. Cell morphology was quantified by manually outlining 10 cells per image per group in ImageJ and obtaining values for maximum Feret diameter (Dmax) of cells and Feret diameter aspect ratio of cells (Dmax/Dmin), where Dmin is the minimum Feret diameter. The total number of evaluated images was 10.

The relative cell number of adherent hMSCs after 24 h of incubation was measured by a calcein AM assay. The multifunctional reader CLARIOstar ® (BMG LABTECH, Germany) was used to analyse the fluorescent intensity. The relative cell numbers were calculated through interpolation via a standard curve.

2.5.3. Cell viability analysis and cell growth on scaffolds

The viability of hMSCs on scaffolds at 1 day of culturing was determined using a cell detachment protocol, described in [16]. The culture medium was removed with a micropipette. Then, scaffolds were placed in new wells and were washed with PBS. After that, 1 mL of trypsin was added. After incubation, 2.5 mL of fresh medium were added and the cell suspension was collected and centrifuged at 1500 rpm for 5 min. Finally, cells from the pellet were counted using a Gorjaev's count chamber and an inverted optical microscope. Trypan blue solution was

used to assess cell viability. This test measured the number of viable cells, based on the concept that viable cells have an intact membrane and trypan blue cannot be incorporated. Dead cells have an altered membrane and take up the dye.

Mesh scaffolds (1×1 cm^2) were transferred into non-adherent 24-well tissue culture plates, onto which hMSCs were slowly inoculated at a density of 1.5×10^5 cell per scaffold. Cells were cultured in a growth medium for 3, 7 and 11 days. Cell proliferation was evaluated on day 3, 7 and 11. The cells at each time point were stained by the Calcein AM (Invitrogen). For this reason, 5 μL of assay reagent was added to each well containing 1 mL of media, and cells on scaffolds were incubated for 30 min at standard culture conditions. Then, confocal microscopy was used to observe the live cells on the scaffolds.

2.5.4. In vitro osteogenic differentiation and mineralization analysis

Induction of differentiation towards the osteogenic lineage was performed using our previously reported protocol [17]. Briefly, each scaffold with cells was treated with an osteogenic medium consisting of DMEM supplemented with 0.1 μM dexamethasone (Sigma-Aldrich, UK), 10 mM β-glycerol phosphate (Sigma-Aldrich, UK) and 0.2 mM ascorbic acid (Sigma-Aldrich, UK). The medium was changed twice weekly. On day 7 of induction, scaffolds with cells were assayed for mineralization by calcein or alizarin red [18]. For calcein staining, the scaffolds were treated with culture medium containing 5 μg/ml calcein overnight at 5 % CO_2/95 % air, 37 °C, washed 2 times with PBS, and examined using confocal microscopy. The quantification of calcium deposits on scaffolds was performed by measuring the fluorescence intensity using multifunctional reader CLARIOstar (485 nm excitation, 530 nm emission). Then, the amount of calcium deposits on scaffolds was calculated through interpolation via a standard curve.

3. Results and discussion

3.1. Scaffolds morphology

Randomly oriented fibrous scaffolds with interconnected porous structure were obtained using a conventional electrospinning process. The scaffolds' morphology and the results of structural evolution such as fibre diameter and the distance between nearby fibres are shown in Fig. 1. A smooth, uniform, bead-free fibre surface is observed for PCL and PHBV polymer scaffolds. The fibre diameter histograms revealed that the majority of fibres in the case of PCL and PHBV scaffolds had a diameter of 4.05 ±1.15 μm and 7.17±1.26 μm, respectively. In the case of PHBV-SiHA scaffolds, the average fibre diameter was 4.11±2.89 μm. It is important to note that the agglomerates of SiHA nanoparticles were also observed on the fibres' surface with the size in the range from 800 nm to 12 μm. As the distance between nearby fibres for all the samples was measured, it was found that the average distance between separate fibres for the PCL scaffolds was 11.74±7.82 μm. For the PHBV and PHBV-SiHA scaffolds, an average distance between nearby fibres was 23.12±15.74 μm and 24.75±18.31 μm, respectively, which resulted in increased porosity.

In Fig. 1 (bottom), SEM images of PHBV-SiHA scaffold revealed that the SiHA nanoparticles concentrated within the fibre, and the average size of the agglomerates was 0.23±0.06 nm. However, the particle agglomerates were also observed on the fibre surface and between nearby fibres. It is likely that they agglomerated while the polymer solution moved towards the spinneret. The content of SiHA nanoparticles within PHBV polymer scaffolds affected the fibre morphology and size distribution. Additionally, SiHA is a non-conductive material, thus it may decrease the charge of the polymer, resulting in a lower stretch of the jet, thereby leading to a decrease of the stretching force at the same voltage and an increase of the fibre diameter. Moreover, fibre formation during the electrospinning process is based on the viscoelastic solution stretching. The viscosity of polymer solution has a direct effect on the fibre size and could be the reason for the differences between the diameter of PCL (μ=1.74) and PHBV (μ=2.36) fibres obtained at the same process parameters [19]. The obtained results confirmed the

advantages of the electrospinning process in the fabrication of highly porous structures designed for the substitution of bone defects. Incorporation of SiHA nanoparticles into the polymer scaffolds structure, on the one hand, allows to form non-uniform fibres in diameter, which may provide a larger surface area to volume ratio and potentially could positively affect the transport of nutrients into the scaffold and cell viability (cellular diameter 5-20 μm) [20].

3.2. FTIR, Raman and XRD characterization

All the spectra of the scaffolds presented in the study were analysed and compared with the spectra obtained for pure SiHA powder (Fig. 2 top left). The FTIR spectra showed several characteristic bands for PCL scaffolds at 1721 cm^{-1} (C=O stretching), 1293 cm^{-1} (C-O and C-C stretching), 1240 cm^{-1} (C-O-C asymmetric stretching), 1185 cm^{-1} (OC-O stretching) and 1165 cm^{-1} (C-O-C symmetric stretching) [21]. The results obtained for PHBV and PHBV-SiHA indicated that chemical functional groups for both samples were very similar. The typical PHBV absorption peaks at 1720 cm^{-1} (C=O stretching), 1276-1452 cm^{-1} (C-H stretching), 1228 cm^{-1} and 1129 cm^{-1} (C-O-C stretching), 1180 cm^{-1} (C-O asymmetric stretching) and 1054 cm^{-1} (C-O symmetric stretching) were detected [22]. In the case of PHBV-SiHA samples, the main vibrational bands are observed at 1028 cm^{-1} (ν_1 P-O symmetric stretching) and 562 cm^{-1} (ν_4 P-O asymmetric stretching). The FTIR results confirmed the presence of SiHA in the structure of polymer PHBV scaffolds.

The results of the Raman spectroscopy are in the agreement with FTIR results and confirm the presence of SiHA in the structure of the polymer PHBV-SiHA scaffolds. Raman spectra of semicrystalline PCL with characteristic bands at 1720 cm^{-1} (νC=O stretching), 1470-1415 cm^{-1} (δC-H stretching), 1304-1281 cm^{-1} (wC-H stretching), 1107-1033 cm^{-1} (skeletal stretching) and 956-866 cm^{-1} (νC-COO stretching) are shown (Fig. 2 top right). For the PHBV scaffold, the major bands were observed at 839 cm^{-1} (νC-COO stretching), 1364 cm^{-1} (δCH_3 stretching), 1451 cm^{-1} (δCH_2 stretching), 1727 (νC=O stretching). The presence of typical Raman intensities for

SiHA powder in PHBV at 962 cm^{-1} (v_1 P-O symmetric stretching) and 1048 cm^{-1} (v_3 P-O asymmetric stretching) was detected.

The XRD data of fibrous scaffolds are presented in Fig. 2 (bottom left). The major peaks specific for PCL are observed at 2θ = 21.3°, 21.9°, 23.7° corresponding to the (110), (111) and (200) planes [23]. XRD pattern of PHBV-SiHA electrospun scaffolds shows characteristic peaks of PHBV at 2θ of 13.6°, 17.1°, 20.3°, 21.7°, 25.7° and 27.3°, which were assigned to the (020), (110), (021), (101), (121) and (040) crystallographic planes of the orthorhombic unit cell, respectively [24]. Additionally, for the same sample, the most prominent peaks corresponding to SiHA were observed at 28.9° (210), 31.8° (211) 32.9° (300) and 35.5° (301) [25]. However, the peaks typical for SiHA between 10° and 28° overlapped with the diffraction peaks of PHBV. Moreover, the peaks of SiHA in PHBV-SiHA composite scaffold became slightly broader and less intensive compared with those for pure SiHA nanoparticles, implying a low number of detected nanoparticles, low crystallinity and smaller crystallite size.

3.3. Wettability

The water contact angle measurements were performed to provide understanding on the influence of SiHA nanoparticles on the polymer scaffolds' chemistry and wettability. The water contact angles are shown in Fig. 2 (bottom right). All fibrous samples demonstrate contact angles of over 100°, which reveals the hydrophobic nature of the scaffolds. The largest contact angle is obtained for PCL scaffold (132.13±1.95°) compared with PHBV scaffold and hybrid scaffold of PHBV-SiHA. It was concluded that the presence of SiHA nanoparticles in the PHBV fibrous scaffold had no significant effect on the contact angle. The contact angle for PHBV-SiHA slightly increased to 125.36±1.61° compared with PHBV (122.55±2.29°). It was expected that due to hydrophilic nature of SiHA nanoparticles used to prepare hybrid scaffolds, the contact angle will be lower for PHBV-SiHA scaffold compared with PHBV. However, due to wettability results obtained in this study, we assume that such parameters as scaffolds porosity and fibers roughness can cause the most pronounced influence on scaffolds wettability. It is reported that

the surface roughness increases with fiber diameter increase and additional content of inorganic inclusions such as HA [46]. It can be clearly seen in Fig. 1 (bottom) that the presence of SiHA nanoparticles and their agglomerates in polymer scaffolds results in changes of the fibers surface roughness and their diameter [47,48]. Since SiHA is hydrophilic and its content does not exceed 10 wt. %, there is an insignificant change of the contact angle for the scaffolds compositions investigated in this paper.

3.4. hMSC adhesion, viability and cell growth on scaffolds

Cell adhesion, viability and proliferation are important aspects in estimation of scaffolds application in tissue regeneration. For a tissue engineering scaffold, surface properties and structure are major factors in regulating cell behaviour and growth [26]. In the current study, we analysed how the structure and surface properties of the scaffolds affected hMSC adhesion, viability, growth and shape. First, the effect of SiHA on hMSC adhesion was investigated. PCL was also analysed as a scaffold with well-known physicochemical properties [27]. As shown in Fig. 3A (left), the relative cell adhesion for PCL and PHBV was almost the same while the relative cell adhesion on the surface of PHBV-SiHA was 1.45 ± 0.3 times greater than that of the PHBV scaffold, indicating the effect of the SiHA nanoparticles. It has been shown that cell adhesion depends on a variety of characteristics of the underlying materials, such as surface profile (roughness, pore size) and wettability, that shift the absorbance of the external cellular matrix (ECM) components and proteins, originating from the serum components of the cultural medium as well as produced by hMSCs. It was shown in previous research that cell adhesion, proliferation and detachment strength are very sensitive to surface roughness [28]. The incorporation of SiHA nanoparticles allows increasing the surface area and enriching the surface with Ca, Si and P, resulting in enhanced adhesion of hMSCs. According to the wettability, it is well-known that poly-3-hydroxybutyric acids and their copolymers are quite hydrophobic polyesters (Fig. 2 bottom right) [29]. The introduction of SiHA nanoparticles containing

nonpolar chemical groups may also play important role in the improved biocompatibility of PHBV for increased cell adhesion of hMSCs on the surface of scaffold.

The important mechanism that can explain the distinct adherence of the hMSCs to various materials is the difference in the amount and types of ECM proteins that are absorbed on the surface of the material. It was shown in previous research that ECM protein absorbance was higher in the nanophase (with grain sizes less than 100 nm) alumina, titania, and hydroxyapatite (HA) and have contributed to the enhanced cell adhesion. This enhanced cell adhesion depends on the surface topography (specifically on grain and pore size) of nanophase ceramics [30]. The mechanism of cell adhesion on poly(lactic-co-glycolic acid) (PLGA) and PCL scaffolds has been compared. The obtained results revealed that hMSCs adhered on PLGA primarily via collagen type I, while vitronectin mediates their attachment to PCL, which also influenced the adherence, morphology and osteogenic differentiation potential of the cells due to various integrin signalling [31].

The viability of hMSCs on three types of scaffolds was investigated after 24 h of incubation. The survival rates of the cells for all three scaffolds after 24 h of incubation were above 82 % (Fig. 3A right). Among these scaffolds, PHBV-SiHA revealed the largest viability of hMSCs (> 95 %), indicating that the most cells were alive. This is a very important criterion for cell growth. These results are in a good agreement with the previous observation of cell adhesion. The initial cell adhesion after 24 h has impact on cell proliferation due to integrin-mediated signalling. In contrast, the loss of cell adhesion leads to cell apoptosis, preventing cell growth [32]. The presented above results clearly demonstrate that the investigated scaffolds are biocompatible and induce cell growth.

To verify that our tested scaffolds, especially PHBV and PHBV-SiHA, were viable substrates for cell growth, hMSCs were cultured on the surface of the scaffolds over 11 days. We stained the cells with calcein AM and imaged them by confocal laser scanning microscopy (CLSM). CLSM images showed that on the first day, the cells were sparsely distributed on the surfaces of the

scaffolds. Long-term cell culture with hMSCs showed that the cells proliferate well on the scaffolds and form a confluent cell layer after 11 days (Fig. 3B). In addition, hMSCs stained by calcein AM adhered on scaffolds at higher magnification can be observed in Supporting Information (Fig. S1).

3.5. hMSC attachments and morphological changes of hMSCs in response to scaffolds (PCL, PHBV and PHBV-SiHA)

Apart from cell adhesion, cell viability and growth, the regulation of cell morphology, including geometric characteristics of cells, is very important aspect, which should be considered. Indeed, for tissue engineering scaffold, surface properties and structure are major factors in regulating cell behaviour and morphology [33]. Therefore, we then examined the influence of structure and surface properties of scaffolds (PCL, PHBV and PHBV-SiHA) on morphological characteristics of adherent hMSCs. The hMSCs were stained with anti-CD90-PE (shown in orange), and CLSM was used to visualize the cell shapes. CLSM images from 24 h incubation demonstrate the adherent hMSCs on surfaces of scaffolds (Fig. 4A). It is clearly seen that the cells became adherent after 24 h of *in vitro* cultivation. These cells bridges between the fibres and integrated with the surrounding mesh of scaffolds. The cell shapes for all three types of scaffolds are different. The cell morphological parameters were analysed quantitatively by ImageJ and presented using maximum Feret diameter (D_{max}) of cells and Feret diameter aspect ratio of cells (D_{max}/D_{min}), where D_{min} is the minimum Feret diameter. The results from the quantification of D_{max} and diameter-based aspect ratio of adhered hMSCs at 24 h are presented in Fig. 5B (top left, top right). The comparison in geometrical characterization of hMSCs showed that hMSCs on the surface of PCL and PHBV-SiHA have significantly higher D_{max} than PHBV; D_{max} of hMSCs on PHBV was smaller than PHBV-SiHA. All analysed cells on PCL and PHBV-SiHA showed an approximate aspect ratio of 2.4 ± 0.4 for PCL and 2.6 ± 0.5 for PHBV-SiHA, which means that, in general, D_{max} was more twice as large as the D_{min}, and the general shape was elliptical. In contrast, the cells attached on PHBV demonstrated aspect ratio of 1.1 ± 0.2 and

have a nearly spherical shape. The fluorescence images in Fig. 5B (bottom) display the hMSCs with an aspect ratio of 2.4 for PCL, 1 for PHBV and 2.6 for PHBV-SiHA. These finding clearly demonstrate how different surfaces of scaffolds have influence on cell shape. This observation is also related to better cell adherence activity of the hMSCs in the case of the PBHV-SiHA. The highly adherent materials that recruits the ECM components that is lead to cells adherence via ECM-integrin connection and signalling may lead to spreader cell morphology compared to cells, which seeded on the surface with restricted activation of integrin signalling. The cell morphology regulates biological processes, such as proliferation, differentiation and the commitment of adult stem cells to specific lineages. An adherent state is necessary for survival of hMSCs, and integrin signalling enhances the proliferative activity of hMSCs [34]. The nanorelief of fibres, which is formed by SiHA nanoparticles in PHBV scaffolds may serve as a support for a strong attachment of the cells to the scaffold's substrate compared to those with smooth surfaces without particles addition [35].

The surface charge constant (d_{33}) for the used in the study hybrid polymers were measured. They were revealed to be 0.605±0.093 pC/N and 1.558±0.065 pC/N for PHBV c/l and PHBV c/l +SiHA, respectively. It is known that non-stoichiometric HA also reveals piezoelectric properties [49], thus we expect that SiHA nanoparticles addition to scaffolds could have contributed in such a way that silicates distorted the lattice of HA which could also generate additional piezoelectric potential in hybrid PHBV-Si-HA scaffolds. Thus, hybrid scaffolds of PHBV-SiHA revealed larger values of d_{33} constants compared with pure PHBV scaffolds. We also measured the piezocharge constants of PCL, which equaled zero.

Cell culture experiments were performed in static conditions, therefore, the effect of piezoelectric nature of the prepared hybrid compounds was difficult to derive and the most pronounced effect on different cell behavior observed in the paper was connected with the addition of SiHA nanoparticles, which resulted in both surface chemistry and topography change of the polymer fibers.

3.6. In vitro osteogenic differentiation of hMSCs and deposition of minerals

The potential to differentiate to the variety of connective tissue cell types, such as osteoblasts, adipocytes and chondrocytes, can be considered as one of the main functional characteristic of hMSCs, which has to be assessed upon cell treatment [36]. Osteoblasts produce bone matrix proteins and they also catalyse the mineralization of bone matrix into bone [37]. For tissue-engineering scaffolds used in bone regeneration, the mineralization ability is key factor, which should be considered. Therefore, we examined the calcium mineralization of hMSCs on scaffolds after 7 days of culture in osteogenic medium. For osteogenic differentiation, we seeded the scaffolds at densities of 0.3×10^6 cells per sample and assessed the deposition of the bone mineral (calcium phosphate) by staining the samples with calcein (Fig. 5) and alizarin red (Supporting Information, Fig. S4). CLSM images showed a green colour in the images, which indicates the presence of the complex formed by calcium ions and the calcein. As it can be clearly seen that positively stained calcein-calcium complexes were accumulated within the cavity (area between separate fibres in scaffolds) of PHBV-SiHA and PHBV after induction of osteogenic medium for 7 days. In contrast, a small number of calcium deposits was displayed in case of PCL. As it was shown previously in [38] calcein labelling of calcium deposits can be used to quantitatively assess the mineral contents *in vitro*. The calcium phosphate densities on all of the PHBV and PHBV-SiHA surfaces were significantly increased compared with PCL surface (Fig. 5), which is the evidence of the possible influence of PHBV piezoelectric nature. The piezoelectric scaffolds have exhibited more favourable cellular attachment and proliferation compared with non-piezoelectric, even in the absence of deformation [7]. It is clearly seen from Fig. 5 (bottom right), the largest mass of deposited calcium (~45 µg) corresponds to the PHBV-SiHA scaffold in comparison with PCL (~10 µg), and PHBV (~23 µg). Similar trends were observed in the case of alizarin red staining, i.e., when scaffolds with cells were stained with alizarin red, PHBV-SiHA showed intense staining, indicating abundant matrix mineralization,

while PCL was only slightly stained (Fig. S3). These findings clearly demonstrate that PHBV-SiHA scaffolds possessed the greatest potential to enhance osteogenic maturation and PHBV-SiHA was good for trapping the minerals. In addition, more images demonstrating the scaffold mineralization during osteogenic differentiation can be found in Supporting Information (Fig. S4). We suppose that the cell substrate adherence and induction of spread morphology may promote the osteogenic lineage commitment and we observed enhanced biomineralization in the case of PHBV-SiHA scaffold.

It is known that the surrounding cellular microenvironment may have a direct or indirect effect on hMSCs behaviour, including adhesion and differentiation processes [39, 40]. Despite the osteogenic activity of SiHA nanoparticles, where calcium favoured enhanced proliferation and morphological changes in hMSCs with the upregulated expression level of osteogenic genes [41, 42], there are several parameters, such as surface roughness and piezoelectric nature of the material, which may play a crucial role in cell behaviour. It is reported that surface roughness can stimulate hMSCs to induce osteogenic differentiation *in vitro* and produce bone mineral [43-45].

Although many details of the hMSC differentiation processes are still unknown, it was shown that the addition of SiHA nanoparticles in the fibre structure of piezoelectric PHBV scaffolds stimulates the attachment and spreading of the hMSCs and significantly increases the differentiation ability of MSCs, which significantly affected the 3D scaffolds' mineralization capability.

4. Conclusion

This cell attachment and differentiation study revealed that hybrid piezoelectric PHBV scaffolds with the addition of SiHA nanoparticles significantly promoted the adhesion of hMSCs

compared with pure piezoelectric PHBV and non-piezoelectric PCL. Calcium assays showed that hMSCs differentiated into osteoblasts; moreover, significantly improved mineralization was observed in the case of hybrid PHBV-SiHA scaffolds. Though the underlying mechanisms responsible for the improved hMSCs adhesion and differentiation require additional investigation, the results obtained in this study allow us to conclude that the hybrid PHBV-SiHA scaffolds reveal superior osteoinductive properties. We suggest that the main reasons for that are connected with the scaffolds' chemistry change due to bioactive Si-HA nanoparticles addition or surface charge change due to inherited PHBV scaffolds piezoelectricity, which require additional investigations. Thus, the results obtained in this study specify the significance of the development of 3D biodegradable PHBV piezoelectric scaffolds with addition of SiHA nanoparticles for bone tissue engineering applications.

5. Acknowledgements and conflict of interest statement

The authors are thankful to Mr M. Syrtanov (General Physics Department, TPU, Tomsk), Professor C. Oehr (Fraunhofer IGB, Stuttgart), and Professor M.V. Chaikina (Institute of Solid State Chemistry and Mechanochemistry SB RAS, Novosibirsk, Russia) for their assistance with the XRD diffraction analysis, polymer solution viscosity measurements, and fabrication of SiHA nanopowder, respectively. This study was supported by the Federal Target Program #14.587.21.0013 (a unique application number 2015-14-588-0002-5599). The authors are thankful to Roman Chernozem (TPU) for piezocharge constants measurements. The authors have no conflict of interest.

References

[1] R.S. Singh, N. Kaur, V. Rana, J.F. Kennedy, Recent insights on applications of pullulan in tissue engineering, Carbohydr. Polym. 153 (2016) 455–462. doi:10.1016/j.carbpol.2016.07.118.

[2] K.E.M. Benders, P.R. van Weeren, S.F. Badylak, D.B.F. Saris, W.J.A. Dhert, J. Malda, Extracellular matrix scaffolds for cartilage and bone regeneration, Trends Biotechnol. 31 (2013) 169–176. doi:10.1016/j.tibtech.2012.12.004.

[3] S. Agarwal, J.H. Wendorff, A. Greiner, Use of electrospinning technique for biomedical applications, Polymer (Guildf). 49 (2008) 5603–5621. doi:10.1016/j.polymer.2008.09.014.

[4] Q.L. Loh, C. Choong, Three-dimensional scaffolds for tissue engineering applications: role of porosity and pore size., Tissue Eng. Part B. Rev. 19 (2013) 485–502. doi:10.1089/ten.TEB.2012.0437.

[5] L. Zhang, Y. Morsi, Y. Wang, Y. Li, S. Ramakrishna, Review scaffold design and stem cells for tooth regeneration, Jpn. Dent. Sci. Rev. 49 (2013) 14–26. doi:10.1016/j.jdsr.2012.09.001.

[6] Z. Rezvani, J.R. Venugopal, A.M. Urbanska, D.K. Mills, S. Ramakrishna, M. Mozafari, A bird's eye view on the use of electrospun nanofibrous scaffolds for bone tissue engineering: Current state-of-the-art, emerging directions and future trends, Nanomedicine Nanotechnology, Biol. Med. 12 (2016) 2181–2200. doi:10.1016/j.nano.2016.05.014.

[7] A.H. Rajabi, M. Jaffe, T.L. Arinzeh, Piezoelectric materials for tissue regeneration: A review, Acta Biomater. 24 (2015) 12–23. doi:10.1016/j.actbio.2015.07.010.

[8] E. Fukada, I. Yasuda, On the Piezoelectric Effect of Bone, J. Phys. Soc. Japan. 12 (1957)

1158–1162. doi:10.1143/JPSJ.12.1158.

[9] C. Ribeiro, V. Sencadas, D.M. Correia, S. Lanceros-Méndez, Piezoelectric polymers as biomaterials for tissue engineering applications, Colloids Surfaces B Biointerfaces. 136 (2015) 46–55. doi:10.1016/j.colsurfb.2015.08.043.

[10] I. Yasuda, Electrical callus and callus formation by electret., Clin. Orthop. Relat. Res. (1977) 53–6. http://www.ncbi.nlm.nih.gov/pubmed/598093 (accessed April 18, 2017).

[11] E. Fukada, Y. Ando, Piezoelectric properties of poly-β-hydroxybutyrate and copolymers of β-hydroxybutyrate and β-hydroxyvalerate, Int. J. Biol. Macromol. 8 (1986) 361–366. doi:10.1016/0141-8130(86)90056-5.

[12] K. Sato, Y. Kumagai, J. Tanaka, Apatite formation on organic monolayers in simulated body environment., J. Biomed. Mater. Res. 50 (2000) 16–20. http://www.ncbi.nlm.nih.gov/pubmed/10644958 (accessed April 18, 2017).

[13] J. Vandiver, D. Dean, N. Patel, C. Botelho, S. Best, J.D. Santos, M.A. Lopes, W. Bonfield, C. Ortiz, Silicon addition to hydroxyapatite increases nanoscale electrostatic, van der Waals, and adhesive interactions, J. Biomed. Mater. Res. Part A. 78A (2006) 352–363. doi:10.1002/jbm.a.30737.

[14] N. Patel, S.M. Best, W. Bonfield, I.R. Gibson, K.A. Hing, E. Damien, P.A. Revell, A comparative study on the in vivo behavior of hydroxyapatite and silicon substituted hydroxyapatite granules., J. Mater. Sci. Mater. Med. 13 (2002) 1199–206. http://www.ncbi.nlm.nih.gov/pubmed/15348666 (accessed February 8, 2016).

[15] N. V. Bulina, M. V. Chaikina, A.S. Andreev, O.B. Lapina, A. V. Ishchenko, I.Y. Prosanov, K.B. Gerasimov, L.A. Solovyov, Mechanochemical Synthesis of SiO_4^{4-} - Substituted Hydroxyapatite, Part II - Reaction Mechanism, Structure, and Substitution Limit, Eur. J. Inorg. Chem. 2014 (2014) 4810–4825. doi:10.1002/ejic.201402246.

[16] S. Palomeras, M. Rabionet, I. Ferrer, A. Sarrats, M. Garcia-Romeu, T. Puig, J. Ciurana, Breast Cancer Stem Cell Culture and Enrichment Using Poly(ε-Caprolactone) Scaffolds, Molecules. 21 (2016) 537. doi:10.3390/molecules21040537.

[17] K. V. Lepik, A.R. Muslimov, A.S. Timin, V.S. Sergeev, D.S. Romanyuk, I.S. Moiseev, E. V. Popova, I.L. Radchenko, A.D. Vilesov, O. V. Galibin, G.B. Sukhorukov, B. V. Afanasyev, Mesenchymal Stem Cell Magnetization: Magnetic Multilayer Microcapsule Uptake, Toxicity, Impact on Functional Properties, and Perspectives for Magnetic Delivery, Adv. Healthc. Mater. 5 (2016) 3182–3190. doi:10.1002/adhm.201600843.

[18] L. V. Hale, Y.F. Ma, R.F. Santerre, Semi-Quantitative Fluorescence Analysis of Calcein Binding as a Measurement of In Vitro Mineralization, Calcif. Tissue Int. 67 (2000) 80–84. doi:10.1007/s00223001101.

[19] D. Zhang, A.B. Karki, D. Rutman, D.P. Young, A. Wang, D. Cocke, T.H. Ho, Z. Guo, Electrospun polyacrylonitrile nanocomposite fibers reinforced with Fe3O4 nanoparticles: Fabrication and property analysis, Polymer (Guildf). 50 (2009) 4189–4198. doi:10.1016/j.polymer.2009.06.062.

[20] S.-M. Lien, L.-Y. Ko, T.-J. Huang, Effect of pore size on ECM secretion and cell growth in gelatin scaffold for articular cartilage tissue engineering, Acta Biomater. 5 (2009) 670–679. doi:10.1016/j.actbio.2008.09.020.

[21] S. Gautam, A.K. Dinda, N.C. Mishra, Fabrication and characterization of PCL/gelatin composite nanofibrous scaffold for tissue engineering applications by electrospinning method, Mater. Sci. Eng. C. 33 (2013) 1228–1235. doi:10.1016/j.msec.2012.12.015.

[22] J. Bitencourt, E. Mendes, M.K. Riekes, V. Matoso De Oliveira, M.D. Michel, H.K. Stulzer, N.M. Khalil, S.F. Zawadzki, R.M. Mainardes, P.V. Farago, PHBV/PCL Microparticles for Controlled Release of Resveratrol: Physicochemical Characterization,

Antioxidant Potential, and Effect on Hemolysis of Human Erythrocytes, Sci. World J. (2012). doi:10.1100/2012/542937.

[23] J.-P. Chen, Y.-S. Chang, Preparation and characterization of composite nanofibers of polycaprolactone and nanohydroxyapatite for osteogenic differentiation of mesenchymal stem cells, Colloids Surfaces B Biointerfaces. 86 (2011) 169–175. doi:10.1016/j.colsurfb.2011.03.038.

[24] M. Scandola, G. Ceccorulli, M. Pizzoli, M. Gazzano, Study of the crystal phase and crystallization rate of bacterial poly(3-hydroxybutyrate-co-3-hydroxyvalerate), Macromolecules. 25 (1992) 1405–1410. doi:10.1021/ma00031a008.

[25] I.R. Gibson, S.M. Best, W. Bonfield, Chemical characterization of silicon-substituted hydroxyapatite., J. Biomed. Mater. Res. 44 (1999) 422–8. http://www.ncbi.nlm.nih.gov/pubmed/10397946 (accessed March 3, 2017).

[26] D. Li, W. Chen, B. Sun, H. Li, T. Wu, Q. Ke, C. Huang, H. EI-Hamshary, S.S. Al-Deyab, X. Mo, A comparison of nanoscale and multiscale PCL/gelatin scaffolds prepared by disc-electrospinning, Colloids Surfaces B Biointerfaces. 146 (2016) 632–641. doi:10.1016/j.colsurfb.2016.07.009.

[27] S.N. Gorodzha, M.A. Surmeneva, R.A. Surmenev, Fabrication and characterization of polycaprolactone cross- linked and highly-aligned 3-D artificial scaffolds for bone tissue regeneration via electrospinning technology, IOP Conf. Ser. Mater. Sci. Eng. 98 (2015) 12024. doi:10.1088/1757-899X/98/1/012024.

[28] D.D. Deligianni, N.D. Katsala, P.G. Koutsoukos, Y.F. Missirlis, Effect of surface roughness of hydroxyapatite on human bone marrow cell adhesion, proliferation, differentiation and detachment strength, Biomaterials. 22 (2000) 87–96. doi:10.1016/S0142-9612(00)00174-5.

[29] S.I. Zubairi, A. Bismarck, A. Mantalaris, The effect of surface heterogeneity on wettability of porous three dimensional (3-D) scaffolds of poly(3-hydroxybutyric acid) (PHB) and poly(3-hydroxybutyric-co-3-hydroxyvaleric acid) (PHBV), J. Teknol. 75 (2015). doi:10.11113/jt.v75.3960.

[30] T.J. Webster, C. Ergun, R.H. Doremus, R.W. Siegel, R. Bizios, Specific proteins mediate enhanced osteoblast adhesion on nanophase ceramics, J. Biomed. Mater. Res. 51 (2000) 475–483. doi:10.1002/1097-4636(20000905)51:3<475::AID-JBM23>3.0.CO;2-9.

[31] S.R. Chastain, A.K. Kundu, S. Dhar, J.W. Calvert, A.J. Putnam, Adhesion of mesenchymal stem cells to polymer scaffolds occurs via distinct ECM ligands and controls their osteogenic differentiation, J. Biomed. Mater. Res. Part A. 78A (2006) 73–85. doi:10.1002/jbm.a.30686.

[32] E.H. Danen, A. Sonnenberg, Integrins in regulation of tissue development and function, J. Pathol. 200 (2003) 471–480. doi:10.1002/path.1416.

[33] D. Li, W. Chen, B. Sun, H. Li, T. Wu, Q. Ke, C. Huang, H. EI-Hamshary, S.S. Al-Deyab, X. Mo, A comparison of nanoscale and multiscale PCL/gelatin scaffolds prepared by disc-electrospinning, Colloids Surfaces B Biointerfaces. 146 (2016) 632–641. doi:10.1016/j.colsurfb.2016.07.009.

[34] J. Kang, H.M. Park, Y.W. Kim, Y.H. Kim, S. Varghese, H.K. Seok, Y.G. Kim, S.H. Kim, Control of mesenchymal stem cell phenotype and differentiation depending on cell adhesion mechanism., Eur. Cell. Mater. 28 (2014) 387–403. http://www.ncbi.nlm.nih.gov/pubmed/25422949 (accessed March 9, 2017).

[35] X. Shi, Y. Wang, D. Li, L. Yuan, F. Zhou, Y. Wang, B. Song, Z. Wu, H. Chen, J.L. Brash, Cell Adhesion on a POEGMA-Modified Topographical Surface, Langmuir. 28 (2012) 17011–17018. doi:10.1021/la303042d.

[36] K. V. Lepik, A.R. Muslimov, A.S. Timin, V.S. Sergeev, D.S. Romanyuk, I.S. Moiseev, E. V. Popova, I.L. Radchenko, A.D. Vilesov, O. V. Galibin, G.B. Sukhorukov, B. V. Afanasyev, Mesenchymal Stem Cell Magnetization: Magnetic Multilayer Microcapsule Uptake, Toxicity, Impact on Functional Properties, and Perspectives for Magnetic Delivery, Adv. Healthc. Mater. 5 (2016) 3182–3190. doi:10.1002/adhm.201600843.

[37] M. Westhrin, M. Xie, M.Ø. Olderøy, P. Sikorski, B.L. Strand, T. Standal, Osteogenic Differentiation of Human Mesenchymal Stem Cells in Mineralized Alginate Matrices, PLoS One. 10 (2015) e0120374. doi:10.1371/journal.pone.0120374.

[38] L. V. Hale, Y.F. Ma, R.F. Santerre, Semi-Quantitative Fluorescence Analysis of Calcein Binding as a Measurement of In Vitro Mineralization, Calcif. Tissue Int. 67 (2000) 80–84. doi:10.1007/s00223001101.

[39] Y. Sun, C.S. Chen, J. Fu, Forcing Stem Cells to Behave: A Biophysical Perspective of the Cellular Microenvironment, Ann. Rev. Biophys. 41 (2012) 519–542. doi:10.1146/annurev-biophys-042910-155306.

[40] J. Barthes, H. Özçelik, M. Hindié, A. Ndreu-Halili, A. Hasan, N.E. Vrana, A. Ndreu-Halili, A. Hasan, N.E. Vrana, Cell microenvironment engineering and monitoring for tissue engineering and regenerative medicine: the recent advances, Biomed Res. Int. 2014 (2014) 921905. doi:10.1155/2014/921905.

[41] A.M.C. Barradas, H.A.M. Fernandes, N. Groen, Y.C. Chai, J. Schrooten, J. van de Peppel, J.P.T.M. van Leeuwen, C.A. van Blitterswijk, J. de Boer, A calcium-induced signaling cascade leading to osteogenic differentiation of human bone marrow-derived mesenchymal stromal cells, Biomaterials. 33 (2012) 3205–3215. doi:10.1016/j.biomaterials.2012.01.020.

[42] Z.-Y. Qiu, I.-S. Noh, S.-M. Zhang, Silicate-doped hydroxyapatite and its promotive effect

on bone mineralization, Front. Mater. Sci. 7 (2013) 40–50. doi:10.1007/s11706-013-0193-9.

[43] M.J. Dalby, N. Gadegaard, R. Tare, A. Andar, M.O. Riehle, P. Herzyk, C.D.W. Wilkinson, R.O.C. Oreffo, The control of human mesenchymal cell differentiation using nanoscale symmetry and disorder, Nat. Mater. 6 (2007) 997–1003. doi:10.1038/nmat2013.

[44] M. Wang, X. Cheng, W. Zhu, B. Holmes, M. Keidar, L.G. Zhang, Design of biomimetic and bioactive cold plasma-modified nanostructured scaffolds for enhanced osteogenic differentiation of bone marrow-derived mesenchymal stem cells, Tissue Eng Part A 20 (2014) 1060-1071. doi: 10.1089/ten.tea.2013.0235.

[45] G. Kumar, M.S.Waters, T. M.Farooque, M. F.Young, C.G. Simon Jr, Freeform Fabricated Scaffolds with Roughened Struts that Enhance both Stem Cell Proliferation and Differentiation by Controlling Cell Shape, Biomaterials 33 (2012) 4022 - 4030. doi: 10.1016/j.biomaterials.2012.02.048.

[46] C. Xu, F. Yang, S. Wang, S. Ramakrishna, *In vitro* study of human vascular endothelial cell function on materials with various surface roughness. Journal of Biomedical Materials Research A 71 (2004) 154-161. doi: 10.1002/jbm.a.30143

[47] M.I. Hassan, N. Sultana, S. Hamdan, Bioactivity assessment of poly (ε-caprolactone)/hydroxyapatite electrospun fibers for bone tissue engineering application, Journal of Nanomaterials 2014 (2014) 8. doi: 10.1155/2014/573238

[48] H. Gert, N. Foley, D. Zwaan, B.J. Kooi, G. Palasantzas, Roughness controlled superhydrophobicity on single nanometer length scale with metal nanoparticles, RSC Advances 5 (2015) 28696-28702. doi: 10.1039/C5RA02348C

[49] E. Fukada, I. Yasuda, On the piezoelectric effect of bone, Journal of the Physical Society of Japan 12 (1957) 1158-1162. doi: 10.1143/JPSJ.12.1158

Figures and tables captions

Fig. 1. SEM images, a histogram of fibre diameter and the distance between nearby fibres for PCL (**top left**), PHBV (**top right**) and PHBV-SiHA (**bottom**) electrospun scaffolds.

Fig. 2. Chemical and phase composition analysis, wettability characterization of pure PCL, PHBV scaffolds and composite PHBV-SiHA scaffold.

Fig. 3. Quantitative analysis of cell adhesion from hMSCs on the scaffolds (PCL, PHBV and PHBV-SiHA) after 24 h of incubation (**A left**). Cell viability analysis of hMSCs on the scaffolds after 24 h of incubation (**A right**). CLSM images of hMSCs on scaffolds after 1 day, 7 days and 11 days of growth (**B**). Values are mean ± SD, n = 3; *P < 0.05.

Fig. 4. CLSM images of hMSCs adhered on the surface of PCL, PHBV and PHBV-SiHA at 24 h. Orange colour indicates anti-CD90-PE-stained membrane (**A**). Geometrical characterization of hMSCs at 24 h: maximum cell diameter (**B top left**) and cell diameter aspect ratio (D_{max}/D_{min}) on (**B top right**) sample surface. Values are mean ± standard error of the means, n = 3. Fluorescence images of cells with district aspect ratios (**B bottom**).

Fig. 5. Deposition of bone mineral (calcium phosphate) on PCL (**top left**), PHBV (**top right**) and PHBV-SiHA (**bottom left**) was demonstrated by calcein green staining during osteogenic differentiation over 7 days. The green colour is an indication of the reaction between calcium ions and calcein green dye. Calcium contents on scaffolds during the osteogenic differentiation (**bottom right**). We seeded the scaffolds at densities of 0.3×10^6 cells per sample. Cavities are shown in red color triangulates. Values are mean ± SD, n = 3; *P < 0.05.

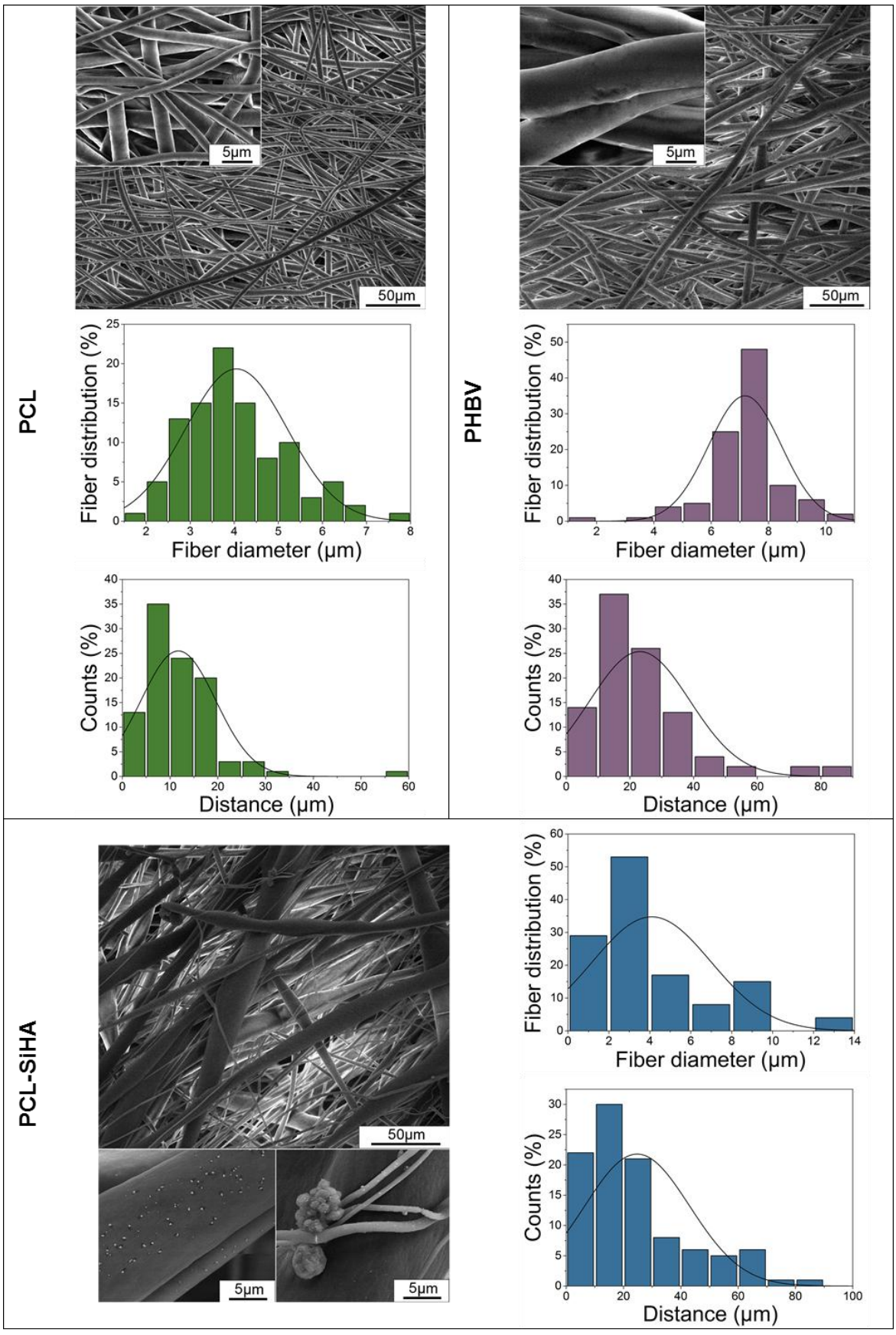
PCL
PHBV
PCL-SIHA
5μm
50μm
Fiber distribution (%)
Fiber diameter (μm)
Counts (%)
Distance (μm)

Fig. 1.

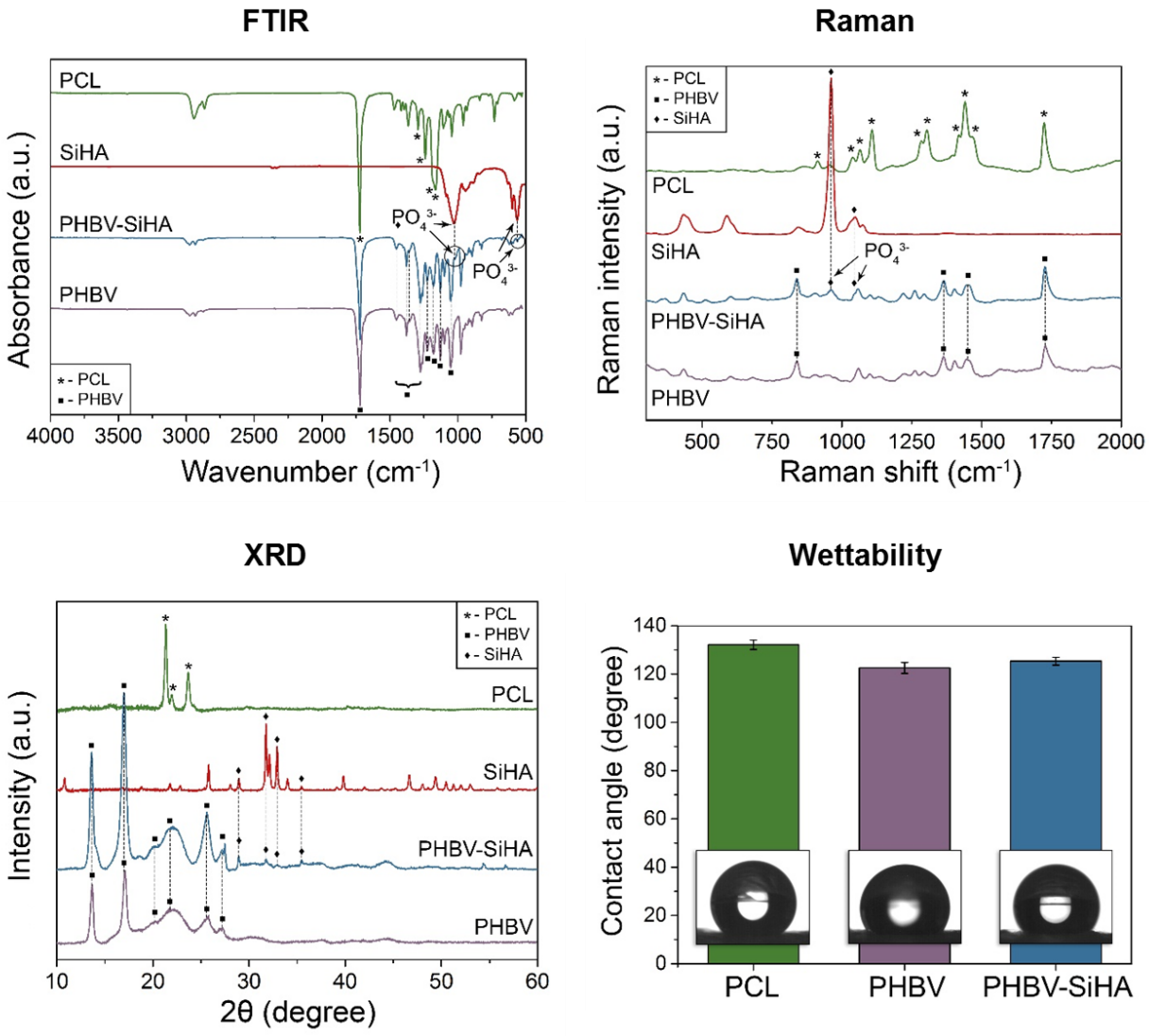
FTIR
PCL
SiHA
PHBV-SiHA
PHBV
PO_4^{3-}
PO_4^{3-}
* - PCL
▪ - PHBV
Absorbance (a.u.)
4000 3500 3000 2500 2000 1500 1000 500
Wavenumber (cm^{-1})
Raman
* - PCL
▪ - PHBV
♦ - SiHA
PCL
SiHA
PO_4^{3-}
PHBV-SiHA
PHBV
Raman intensity (a.u.)
500 750 1000 1250 1500 1750 2000
Raman shift (cm^{-1})
XRD
* - PCL
▪ - PHBV
♦ - SiHA
PCL
SiHA
PHBV-SiHA
PHBV
Intensity (a.u.)
10 20 30 40 50 60
2θ (degree)
Wettability
Contact angle (degree)
0 20 40 60 80 100 120 140
PCL
PHBV
PHBV-SiHA

Fig. 2.

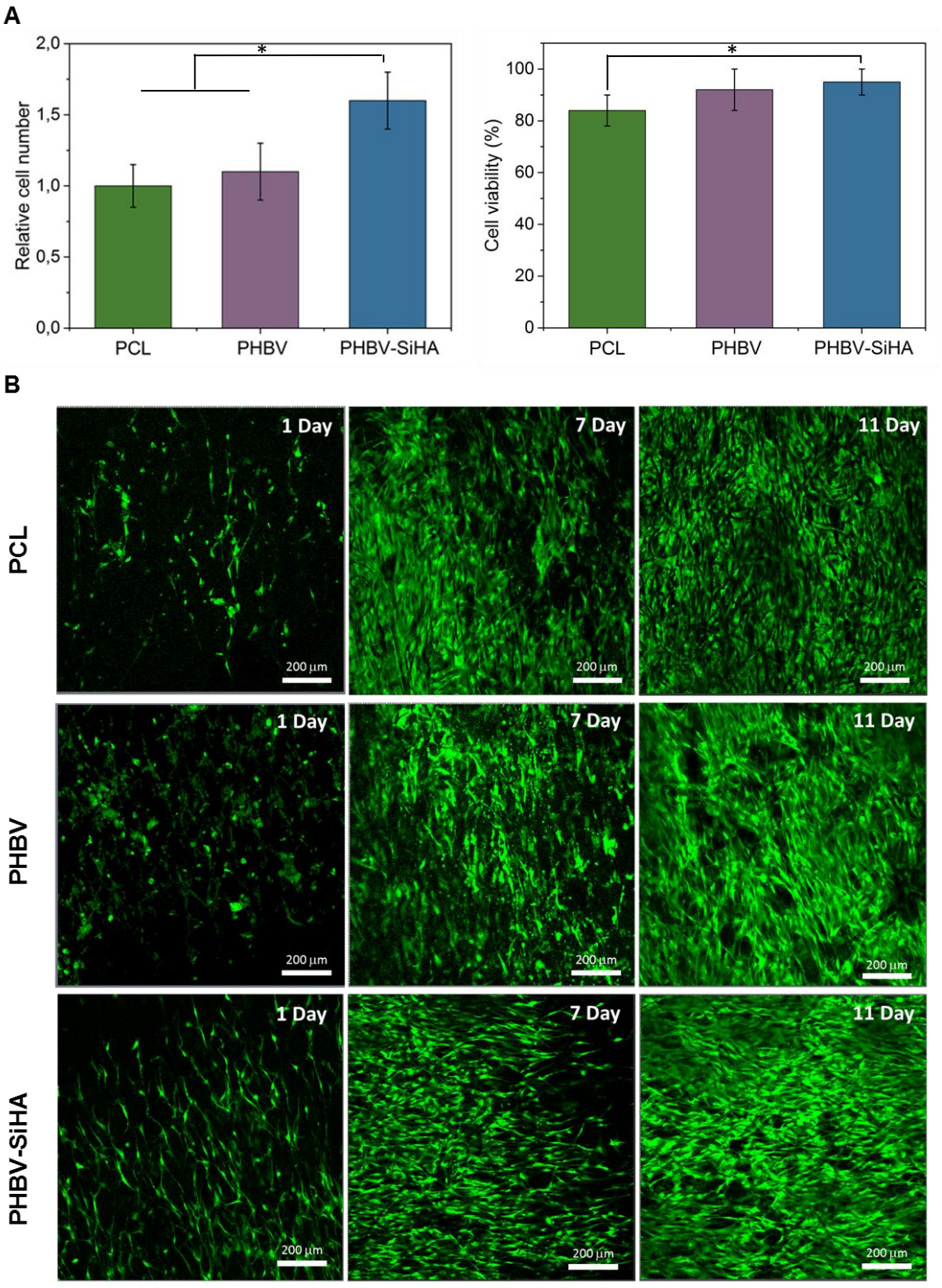
A
Relative cell number
2,0
1,5
1,0
0,5
0,0
*
PCL
PHBV
PHBV-SiHA
Cell viability (%)
100
80
60
40
20
0
*
PCL
PHBV
PHBV-SiHA
B
PCL
PHBV
PHBV-SiHA
1 Day
7 Day
11 Day
200 µm

Fig. 3.

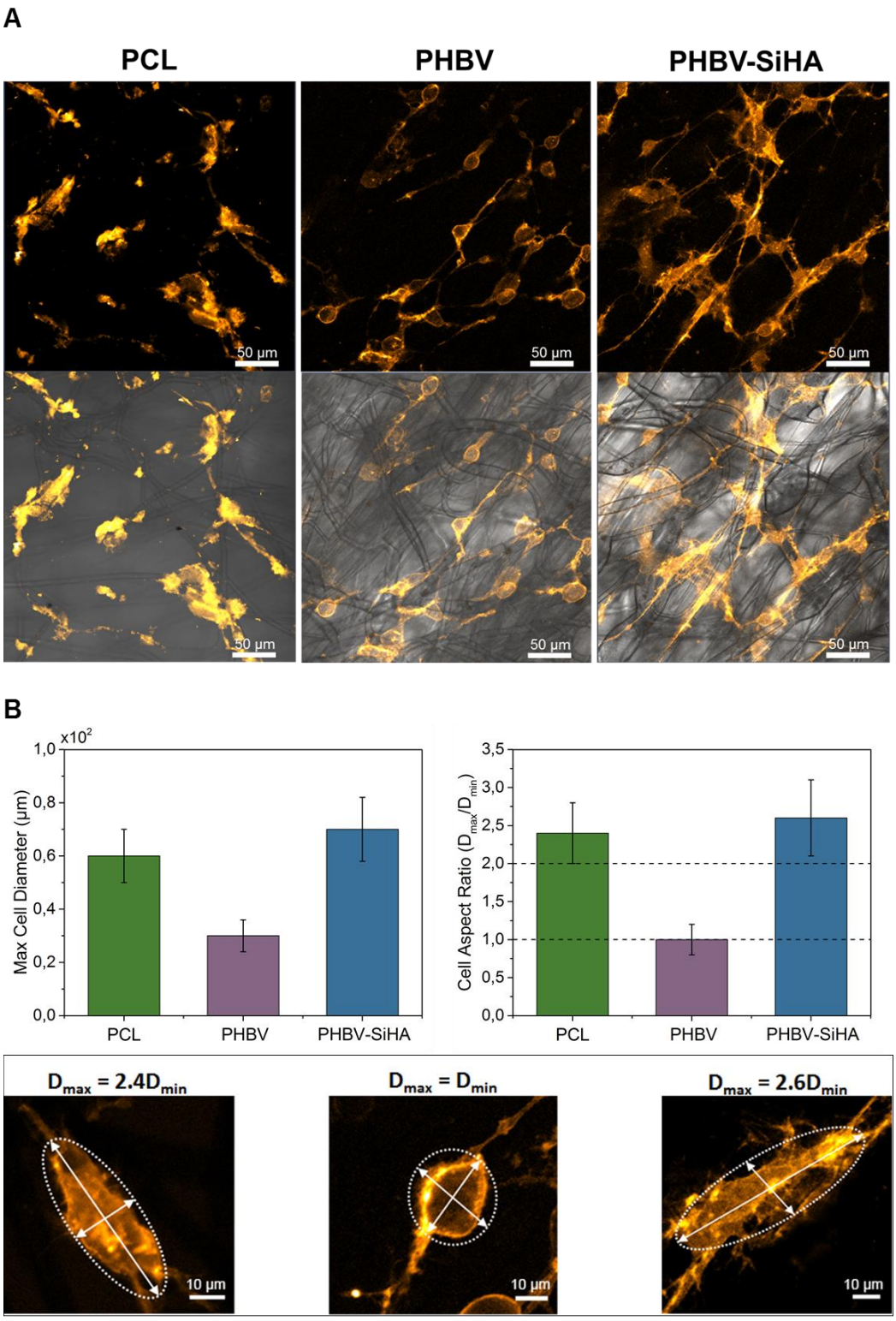
A
PCL
PHBV
PHBV-SiHA
50 µm
B
x10²
Max Cell Diameter (µm)
1,0
0,8
0,6
0,4
0,2
0,0
PCL
PHBV
PHBV-SiHA
Cell Aspect Ratio (Dmax/Dmin)
3,5
3,0
2,5
2,0
1,5
1,0
0,5
0,0
Dmax = 2.4Dmin
Dmax = Dmin
Dmax = 2.6Dmin
10 µm

Fig. 4.

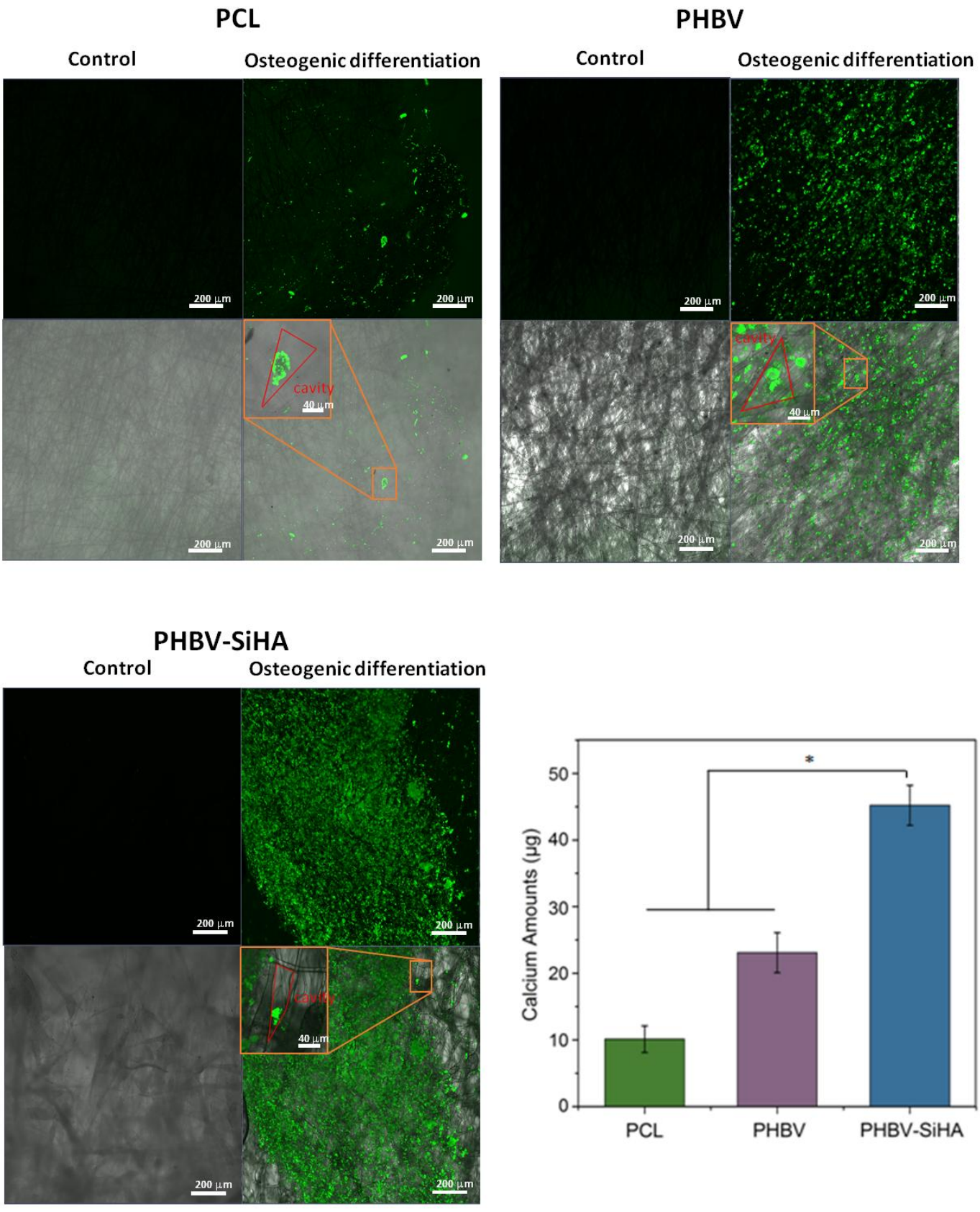
PCL
Control
Osteogenic differentiation
PHBV
Control
Osteogenic differentiation
PHBV-SiHA
Control
Osteogenic differentiation
200 μm
40 μm
cavity
Calcium Amounts (μg)
0
10
20
30
40
50
*
PCL
PHBV
PHBV-SiHA

Fig. 5.

Supplementary Material

Click here to download Supplementary Material: Suplementary materials_submitted.docx

Figure(s)

ELSEVIER
Language Editing Services

Registered Office:
Elsevier Ltd
The Boulevard, Langford Lane,
Kidlington, OX5 1GB, UK.
Registration No. 331566771

To whom it may concern

The paper "A comparison study between electrospun polycaprolactone and piezoelectric poly(3-hydroxybutyrate-co-3-hydroxyvalerate) scaffolds for bone tissue engineering" by Roman Surmenev was edited by Elsevier Language Editing Services.

Kind regards,

Biji Mathilakath
Elsevier Webshop Support

(This is a computer generated advice and does not require any signature)